HHS Public Access

Author manuscript

Adv Drug Deliv Rev. Author manuscript; available in PMC 2019 April 15.

Published in final edited form as:

Adv Drug Deliv Rev. 2018 January 15; 124: 34–49. doi:10.1016/j.addr.2017.11.001.

Mucus models to evaluate the diffusion of drugs and particles

Jaclyn Y. Lock[a], **Taylor Carlson**[b], and **Rebecca L. Carrier**[a,b,*]

[a]Department of Bioengineering, Northeastern University, Boston, Massachusetts, USA

[b]Department of Chemical Engineering, Northeastern University, Boston, Massachusetts, USA

Abstract

Mucus is a complex hydrogel that acts as a natural barrier to drug delivery at different mucosal surfaces including the respiratory, gastrointestinal, and vaginal tracts. To elucidate the role mucus plays in drug delivery, different *in vitro*, *in vivo*, and *ex vivo* mucus models and techniques have been utilized. Drug and drug carrier diffusion can be studied using various techniques in either isolated mucus gels or mucus present on cell cultures and tissues. The species, age, and potential disease state of the animal from which mucus is derived can all impact mucus composition and structure, and therefore impact drug and drug carrier diffusion. This review provides an overview of the techniques used to characterize drug and drug carrier diffusion, and discusses the advantages and disadvantages of the different models available to highlight the information they can afford.

Graphical abstract

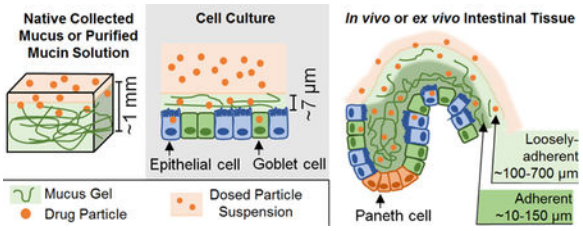

Keywords

Mucosal Drug Delivery; Mucus Penetration; Native Mucus; Mucin Purification; Mucus Composition; Mucus Structure; Animal Models

1. Introduction

The gastrointestinal, respiratory, and vaginal tracts are all lined with a protective mucus layer that is composed of water, proteins, lipids, salts, and cellular debris[1, 2]. The main

*Corresponding Author, rebecca@coe.neu.edu.

structural component of the mucus layer is mucin, a highly glycosylated protein with oligosaccharide side chains including terminal sialic acid and sulfate residues that give mucin its negative charge (Fig. 1)[1, 2]. Mucins can physically and chemically (i.e. via intermolecular interactions) interact with each other and with other components of mucus to form a mesh-like structure (average pore size 10–500 nm)[3–5]. In addition to this mesh-like structure, mucus clearance and binding interactions can regulate microbe penetration, as well as drug and particle diffusion to the underlying epithelium[6, 7]. Thus, it is important to characterize the impact of mucus on drug or drug carrier diffusion to understand the significance of this barrier to drug delivery. As it is not always convenient to directly study the diffusion through the mucosal barrier *in situ* (e.g., within the human gastrointestinal tract), model *in vitro, ex vivo*, and *in vivo* systems can be employed. The ideal mucus model should recapitulate the composition and structure of native human mucus to the greatest extent possible; however, the selection of a model system may be limited by the ease of use, reproducibility, and ability to obtain specific measurements.

When considering model systems for studying drug or drug carrier transport through mucus, one complicating factor is the varied nature of the mucus barrier *in vivo*. Specifically, spatial organization of the mucus layer and its role are unique to the anatomical location (Fig. 2)[9]. In the stomach, the epithelium is lined with mucus and lipid layers which protect against gastric acid and enzymes[10]. In the respiratory tract, periciliary, mucus, and surfactant layers filter out inhaled particulates[11]. In both intestinal and vaginal tracts, an adherent and loosely adherent mucus layer regulates microbe and sperm motility, respectively[12–15]. The properties of cervical mucus and its amount also varies depending on animal species[14, 16]. Drug and particle diffusion are also directly impacted by source specific differences in mucus thickness, and mucin type and glycosylation[17–20]. Reported mucus thickness values in small and large intestine range from 10–750 μm in humans and 100–800 μm in rats[12, 21–23]. In mice, the glycans on the main secreted stomach mucin (Muc5ac) were found to be about half neutral, with many monosulfated, but few fucosylated or sialylated glycans. In contrast, the main colonic mucin (Muc2) is dominated by fucosylated glycans and contains abundant negatively-charged sialylated and sulfated glycans[24]. Human cervicovaginal mucin has an increase in the amount of sialylated and sulfated glycans during ovulation[25–27].

Age can also impact mucus thickness and composition. For example, rat gastric mucus thickness increased from 52 μm at 3 days old to 97 μm at 8 weeks old[29]. Newborn rat small intestine (~24 hours old) glycoprotein composition differed markedly from that of adult rat (> 2 month old)[30]. Specifically, fucose, mannose, galactose, N-acetylgalactosamine, and sulphate concentrations were lower in newborn rat pups compared to adult rats, while N-acetyglucosamine and N-acetylneuraminic acid concentrations were similar. Similar differences were observed between newborn (0 day) and mature (180 days) porcine colonic mucins, where older pigs had higher fucose and lower protein content[31]. In the same study, significantly higher fucose and glucosamine and lower sulfate amounts were observed in mucus from sow-fed vs. formula-fed 21 day old pigs, highlighting the potential significance of diet in impacting mucus composition. As chemical and physical differences in mucus can impact barrier properties, careful selection of a model system for

studying transport through mucus is essential for understanding the potential significance of the mucus barrier to drug delivery in humans.

A variety of mucus models, including native collected mucus, purified mucin preparations, *in vitro* cell cultures, and intact mucosal tissues (studied both *ex vivo* and *in vivo*), have been utilized to study the diffusion of drugs and particles. Mathematical models used to analyze diffusion through complex gel systems[32–36] can be applied to investigate the heterogeneous nature of the mucus gel on different time and length scales[37]. Experimental techniques such as multiple particle tracking (MPT) and fluorescence recovery after photobleaching (FRAP) track diffusion on short time and length scales, while penetration and bulk diffusion studies are on longer time and length scales. It is important to note that results for diffusion coefficients may not be the same due to the heterogeneity of the mucus gel at different scales. Herein, we evaluate the advantages and disadvantages of the different mucus models and what they can be utilized to study. We highlight findings from studies utilizing these different mucus models to demonstrate the information that can be obtained with these systems.

2. Isolated Mucus Models

2.1. Native Mucus Collection and Use

Mucus can be collected from tissues and used directly for transport studies in a variety of experimental configurations. Reported protocols for collecting mucus vary depending on anatomical source. For example, gastrointestinal mucus is gently scraped from the mucosal surface of excised tissue[3, 38], respiratory mucus is collected using an endotracheal tube[39, 40], and vaginal mucus is collected using aspiration or a menstrual collection device[41, 42]. The storage of native mucus at −20 °C does not result in considerable loss of rheological properties[43–45]. Native collected mucus has been employed in experimental techniques including multiple particle tracking (MPT)[3, 38, 46, 47], fluorescent recovery after photobleaching (FRAP)[48–51], penetration studies[52–55], and bulk diffusion studies[53, 56].

MPT is a non-invasive technique in which the diffusion of fluorescently labeled particles is tracked in a medium of interest (i.e. mucus gel) using fluorescence video microscopy [3, 38, 46]. An image analysis algorithm (e.g., MATLAB, ImageJ) is used to detect particle trajectories, allowing quantification of particle dynamics through calculation of ensemble time-averaged mean squared displacement (<MSD>) and effective diffusivity. Microrheological analysis of trajectories can reveal mucus gel properties including microviscosity, elasticity, and heterogeneity of the local micro-environment[47, 57, 58]. As MPT relies on the analysis of particle motion, this method can be used to probe the microenvironment within mucus, as opposed to standard rheological techniques that analyze bulk, macroscopic properties. The particles used in MPT studies can represent drug carriers or drug particles, and as such, this technique provides direct information related to penetration of drug carriers through mucus barriers. The particle surface properties (e.g., chemistry and charge) and particle size can be varied to reveal the significance of these parameters on transport through the mucus barrier[59]. One advantage to carrying out MPT studies on native collected mucus, as opposed to cell cultures or excised tissue as described

below, is the relative ease of focusing on the particles within a thick (e.g., ~1 mm) mucus gel layer, without concern about whether the particles being imaged are within mucus as opposed to the fluid above or cells below the mucus layer. MPT studies on collected porcine intestinal mucus were used to reveal impact of age on mucus barrier properties. 500 nm carboxylate-modified fluorescent polystyrene beads were immobilized ~70% and 99.4% in piglet and adult pig intestinal mucus, respectively[60]. The difference in particle diffusion was attributed to the higher viscosity and DNA content in the pig mucus compared to the piglet mucus. When piglet and pig mucus specimens were treated with DNase, the percent of immobilized particles decreased to 23% and 36%, respectively. MPT also revealed that treating respiratory tract sputum collected from individuals with cystic fibrosis (CF), a disease characterized by increased mucus viscosity[61], with 20 mM of the mucolytic agent N-acetyl cysteine (NAC) decreased mucus viscoelasticity and increased diffusion transport rate of 200 nm polyethylene glycol (PEG)ylated particles 10-fold (Fig. 3)[62]. MPT was also used to demonstrate that stimuli associated with food ingestion can impact the diffusion of model drug carriers in mucus[63]. Increased lipid and Ca^{2+} concentrations, and decreased pH affected the local mucus microenvironment, decreasing amine-, carboxylate-, and sulfate-modified 200 nm particle transport rates and altered porcine intestinal mucus structure[59].

FRAP is another technique that can be used for quantitative analysis of diffusion (e.g., estimation of diffusion coefficient) through collected mucus gels. While MPT enables analysis of diffusion of particulate species, FRAP enables analysis of diffusion of molecules (e.g., proteins) as well as colloidal species (e.g., bile salt micelles, viruses, and other particles) too small to be detected by MPT[48, 49]. A caveat of this technique is the requirement for the species being tracked to be fluorescent, which can be accomplished via conjugation or incorporation of a fluorophore, if it is not likely to significantly alter the diffusion coefficient of the species of interest. In a FRAP experiment, fluorescent probes are added to the mucus sample, a high intensity beam is used to bleach a part of the sample, and recovery of fluorescence of the sample area is monitored. FRAP analysis demonstrated that diffusion of antibodies (IgG, IgA, and IgM) was slowed 3- to 5- fold due to low-affinity interactions within a mucus gel relative to diffusion in distilled water[48]. FRAP analysis also showed that model bile salt micelle diffusion was slowed 3-fold in mucus relative to buffer, while diffusion of molecular species that comprise bile micelles was not affected[49], indicating that bile micelles likely stay intact within the mucus barrier.

Native collected mucus can also be used to study the bulk diffusion of particles or molecules utilizing capillary tubes or membranes. In contrast to MPT, which is utilized to study single particle dynamics, capillary tubes are used to study bulk particle transport into the mucus gel. Again, the diffusing entity must be detectable, for example by fluorescence or radiolabel imaging, or by analytical techniques (e.g., high-performance liquid chromatography). Cervical vaginal mucus was loaded into a capillary tube, sealed on one end, and immersed into a suspension of poly(vinyl alcohol) (PVA) particles loaded with Nile Red (0.5% w/v) [56]. PVA polymers with different molecular weight and degree of hydrolysis (i.e. proportion of ester:hydroxyl groups) were used to synthesize particles with different degrees of muco-adhesivity. Particle size ranged from 230–280 nm, with a higher molecular weight PVA resulting in larger particle size. Using MPT, the PVA particles were characterized as

mobile or adhesive based on their mobility through mucus as compared to adhesive carboxylate-modified particles and mobile PEGylated particles. Mobile and adhesive PVA particles had a zeta potential of approximately −4 and −18 mV, respectively. After a certain time, the capillary tube containing mucus and particles was washed to remove PVA particles that did not penetrate into the mucus gel and then placed in an extraction solution to remove Nile Red, which was quantified by high performance liquid chromatography to determine extent of particle diffusion. Mucoadhesive particles (higher degree of hydrolysis) were unable to penetrate, whereas mobile particles were able to diffuse into the mucus gel. In another study, cervical mucus was loaded into a capillary tube to study the diffusion of poly(lactic-co-glycolic acid) (PLGA) particles containing Coumarin 6, a fluorescent dye[53]. The fluorescence intensity profile was imaged and quantified at different time points, and then fit to a Fickian diffusion model of a solute in a semi-infinite medium by finite element model. PEGylated PLGA particles (100–400 nm in diameter) had a net-neutral charge, and thus reduced electrostatic interactions with negatively-charged mucin fibers and a greater effective particle diffusion coefficient relative to non-PEGylated particles. Penetration of fluorescent particles through a native collected mucus gel can also be monitored using confocal microscopy[52]. A micropump nebulizer was used to aerosolize 100, 200, or 500 nm fluorescent carboxylate-modified nanoparticle suspensions onto native collected porcine pulmonary mucus (~40 μm thick) stained with fluorescent wheat germ agglutinin, which binds to mucin sugars N-acetyl-D-glucosamine and sialic acid. After aerosol deposition, only 100 nm nanoparticles were able to diffuse a measurable distance within the mucus layer (~ 30 μm). Both 200 and 500 nm nanoparticles were size-excluded and were unable to diffuse into the pulmonary mucus.

Cell culture inserts (e.g., Transwells®) and dialysis membranes have also been used to monitor bulk drug and particle diffusion through collected mucus separating two fluid compartments, for example from an apical (donor) to a basolateral (acceptor) compartment of a cell culture well. One important consideration in these studies is that the membrane itself can act as a barrier to diffusion. Careful selection of filter material and cutoff size is important to prevent clogging and minimize loss of mucus during the experiment. This mucus model and setup has been used to study the influence of size, surface charge and hydrophobicity on particle diffusion through mucus The diffusion of paclitaxel (Ptx) through porcine intestinal mucus placed in a cell culture insert (mucus thickness ~446 μm) was enhanced when loaded into 55 nm lipid nanocapsules[54]. Although porcine intestinal mucus from two different animals had different water content (90.8% compared to 87.6%), resulting in different shear and elastic moduli, the apparent permeability (P_{APP}) of Ptx through mucus was similar for the two mucus samples. Drug carrier size impacted transport across mucus loaded in a cell culture insert, where 70% of 12 nm diameter self-nanoemulsifying drug delivery systems (SNEDDs) crossed the mucus layer (929 ± 115 μm) compared to 8% of 456 nm diameter SNEDDs[64]. Mucus can also be sandwiched between two cellulose nitrate filters[45] or polycarbonate filters[65] such that it separates donor and acceptor chambers in a setup similar to a cell culture insert. Diffusion of the short chain fatty acid butyrate was slower in mucus from distal colon, which had higher fucose concentration and lower water content relative to mucus from proximal colon[45].

2.2. Preparation and Characterization of Purified Mucin Solutions

While native collected mucus represents the composition and structure of mucus *in vivo*, the complex, undefined, and highly variable composition can make it difficult to interpret experimental results with respect to potential interactions between a diffusing entity of interest (e.g., drug carrier) and the mucus gel. For example, there was a 25-fold difference between the highest and lowest viscosity values measured in intestinal mucus samples collected from six different pigs[66]. Reconstituted purified mucin solutions are relatively defined in composition, enabling a clearer interpretation of how observations relate to molecular properties and interactions (e.g., enhanced barrier properties with respect to positively charged particles relating to electrostatic interactions with negatively-charged mucin sugars). As purified mucin can be purchased or prepared in bulk and reconstituted in solution as needed, batch-to-batch variability can be minimized. Moreover, as purified mucins are generally available in powdered forms, the reconstitution solution properties (e.g., ionic strength, composition, etc.) can be varied to allow exploration of the impact on mucus gel properties. Mucin gels are often reconstituted in solutions designed to mimic native mucus content (e.g., via inclusion of lipids)[66–68]. However, even with the addition of some components present in native mucus, purified mucin gels may not recapitulate the complex composition, structure and transport properties of native mucus. In addition, if proper precautions are not taken during mucin purification, mucin degradation can occur, with associated changes in rheological properties (i.e. gel-forming capability)[68].

There are a variety of commercially available purified mucin types that have been used to prepare mucin solutions and gels (Table 1). Rheological properties (i.e. viscosity, and storage, loss, and complex moduli) of Sigma mucin solutions reconstituted in phosphate buffered saline (10–60% wt/wt mucin) were lower than those of native collected pig gastric mucus (~5% mucin)[70]. These results indicate that the purified Sigma mucin is structurally not comparable to native mucus, likely due to protease degradation and associated changes in mucin-mucin interactions. It is also likely that the other components of mucus removed during the mucin purification process interact with mucins and alter mucin-mucin interactions and associated rheological properties. Differences between reconstituted Sigma mucin and native collected intestinal mucus are apparent in drug and particulate diffusion experiments[38, 44]. For example, the diffusion of radiolabeled model drugs (glucosamine, glucuronic acid, glucose, metoprolol, antipyrine, propranolol, hydrocortisone, and testosterone) was studied by loading a plastic syringe containing mucus with diffusion media, adding radio-labeled drug, and incubating at 37 °C for 20–50 hours[44]. The contents of the syringe were divided into 10 portions and analyzed for radioactivity. Drug diffusion through reconstituted 1.5% Sigma gastric mucin in 10 mM phosphate buffer was similar to diffusion in phosphate buffer, but faster than diffusion in native collected intestinal mucus. The different drug diffusion rates were attributed to the higher osmolality present in native collected mucus compared to the reconstituted Sigma gastric mucin. Diffusion rates of lipophilic drugs, in particular, were lower in native collected mucus, potentially due to their interaction with hydrophobic components of the mucus gel that could be lost during mucin purification. There has been reported variability and presence of nonmucin proteins (i.e. albumin, secretory immunoglobluins, lysozyme, and proline-rich proteins) in different batches of bovine submaxillary gland mucin and porcine gastric mucin[79]. Since Sigma

mucin contains non-mucin proteins, further purification using a Sephacryl S-1000 superfine column has been used to remove the contaminants[79].

Reconstitution of purified mucin in a chemically relevant solution is essential to mimic the physicochemical properties of native mucus. A simulated vaginal mucus (SVM) was developed to study the diffusion of drugs and particles through a fluid that was similar in pH and osmolarity to native fluid[67, 71]. The SVM was composed of 0.5% glucose, 0.4% sodium chloride, 0.2% lactic acid, 0.1% potassium hydroxide, 0.1% acetic acid, 0.04% urea, 0.02% calcium hydroxide, 0.02% glycerol, and 1.5% wt/vol Sigma gastric mucin in water, and had similar viscosity to mid-cycle cervicovaginal fluid. MPT technique was used to track the diffusion of dapivirine-loaded polycaprolactone particles in SVM, where negatively-charged particles (modified with poloxamer 338 NF or sodium lauryl sulfate) diffused faster than positively-charged particles (modified with cetyltrimethylammonium bromide). A biosimilar intestinal mucus was proposed which contained 0.4% wt/wt Sigma gastric mucin, 3.0% lipid mixture (82% linoleic acid, 12% cholesterol, and 6% soybean phosphatidylcholine), 3.1% serum albumin, 3.1% immunoglobulin G, and 0.5% calf thymus DNA in 10 mM phosphate buffer with 0.75% Tween 80 and 0.04% sodium azide[68]. Diffusion of drugs (metoprolol, propranolol, hydrocortisone, and testosterone) through the biosimilar mucus compared more favorably with diffusion in porcine intestinal mucus than diffusion in Sigma mucin reconstituted in water. The differences in diffusion rates were attributed to the possible loss of the gel-forming ability of Sigma gastric mucin[68], which limits the ability of biosimilar mucus to emulate native mucus rheological properties.

Purification procedures have been developed to isolate mucin from native mucus with minimal degradation of mucin glycoproteins. For example, one extraction procedure begins with homogenization of small intestinal or gastric mucus with 0.2 M sodium chloride containing protease inhibitors and sodium azide, followed by cesium chloride (CsCl) density gradient centrifugation, dialysis, lyophilization, and finally dissolution in 10 mM sodium phosphate and 10 mM sodium succinate buffer (1–50 mg/mL)[73]. Mucin solutions prepared in this manner formed a viscoelastic gel at 25 mg/mL, which corresponds to a physiologically relevant concentration of gastrointestinal mucus (~2.5% wt/wt). When the pH of the mucin solution was dropped from 6.5 to 1, which is representative of the acidic stomach environment, the mobility of 505 nm carboxylate-modified microspheres within the gel was reduced, and the viscosity increased 100-fold. Another purification method utilizes Sepharose CL2B chromatography together with CsCl density gradient ultracentrifugation to isolate mucins[80–82]. When gastric mucus was purified using Sepharose CL2B chromatography, the product contained mucins (i.e. MUC5AC, MUC2, MUC5B, and MUC6) and non-mucin proteins (i.e. histones, actin, and albumin)[83]. The partially purified mucin was reconstituted in distilled water (1% w/v) buffered with 20 mM HEPES buffer at pH 7 and added on top of human cervical (HeLa) cells seeded in a 96-well plate. This mucin solution reduced the number of human papilloma virus type 16 (HPV-16) infected HeLa cells compared to 1% Sigma gastric mucin solution and HEPES buffer control. MPT was used to track the diffusion of fluorescently labeled HPV-16 viruses in the prepared gastric mucin solution. HPV-16 diffusion was hindered when pH was decreased from 7 to 3 due to gel compaction and shrinkage[28, 83]. Similarly, pulsed field gradient-nuclear magnetic resonance (PFG-NMR) has also been used to monitor the diffusion of PEG molecules

through 5 wt% purified gastric mucin in phosphate buffered saline at a pH of 1, 4, or 7.4[82]. PEG was selected as the probe molecule since it has no specific interactions with the mucus gel, is represented by a single sharp band in the NMR spectra, and is readily available in multiple molecular weights. Results showed that mucin structure varied primarily with pH rather than salt concentration and temperature. At neutral pH, the mucin molecules form a homogeneous and porous network, while at pH 1 they form a collapsed heterogeneous network with polymer-dense and water-rich areas. It has been proposed that the changes in mucus properties observed at low pH (representative of gastric conditions) result from disruption of salt bridges in non-glycosylated, cysteine-rich regions of mucin molecules, and associated exposure of hydrophobic protein regions that can then participate in mucin-mucin interactions. The salt bridges, formed between negatively charged carboxylates and positively charged amino groups of amino acid side chains, are broken when negatively charged carboxylates are protonated at low pH, leading to aggregation of mucin fibers[84, 85].

Similar to the purification of gastrointestinal mucins, mucin can be isolated from mucus samples collected throughout the ovulatory menstrual cycle[26, 27, 86, 87]. In one purification process, cervical mucus was centrifuged to remove insoluble components, lyophilized, and the nondialyzable solids were reconstituted in 0.22 M sodium thiocynate with 0.1 M Tris at pH 7.5. Mucin concentration and composition was affected by the ovulatory phase; there was an increased amount of purified mucin during ovulatory phase (~51%) compared to follicular (~25%) and luteal (~31%) phases and sialic acid content was increased in pregnancy mucin compared to preovulatory and postovulatory mucin[27]. Increased mucin concentration correlated with increased storage modulus as measured by a magnetic microrheometer.

Purified mucin preparations offer the possibility of measuring interactions between drug or drug carriers and mucins. Isothermal titration calorimetry (ITC), a technique which measures the heat released or absorbed during a biomolecular binding event[88], revealed that binding of PLGA-PEG nanoparticles (~100 nm) with Sigma bovine submaxillary gland mucin decreased as a function of conjugated PEG concentration (0–25 wt% PEG). Dynamic light scattering was also used to determine interactions between Sigma gastric mucin and negatively- or positively-charged silica nanoparticles (10–15 nm diameter)[89]. Solutions containing nanoparticle only, mucin only, and nanoparticle mixed with mucin were analyzed at 37 °C with a scattering angle of 173 degrees. Positively-charged silica particles increased in size when mixed with mucin, indicating an electrostatic interaction between positively-charged particles and negatively-charged mucin, while negatively-charged silica particles had no change in particle size when mixed with mucin, indicating no binding interaction.

3. Incorporation of Mucus or Mucus-Producing Cells in *In vitro* Cell Culture Models

As an alternative to native collected and purified mucus, cell lines that secrete mucus can be used to study drug and particulate diffusion. These systems may offer the advantage of a more physical representation of the mucus layer being in direct contact with underlying

cells. *In vivo* mucus properties change with proximity to the underlying epithelium (as mentioned previously)[10–13], and these effects may be captured by some *in vitro* cell culture systems. In contrast, the analyses of diffusion through native collected and purified mucus noted above inherently treat mucus as an isotropic medium. Cell cultures that secrete mucus can be grown on cell culture inserts (e.g., Transwell® inserts) to enable determination of drug and particle diffusion from the apical (donor) compartment, through the mucus layer and the cell monolayer, to the basolateral (acceptor) compartment (Fig. 4A)[90]. Drug concentration in the apical and basolateral compartment can be quantified by different analytical techniques including measurement of radioactivity or fluorescence, mass spectrometry or high-performance liquid chromatography. During these experiments, the impact of drugs and drug particles on cell monolayer integrity and tight junctions can be monitored via measurement of transepithelial electrical resistance (TEER). In such studies, both mucus and cells are contributing to the overall tissue barrier, and it can be challenging to assess the impact of each. Cell culture models also allow investigation of the impact of drugs and other stimuli on mucus secretion, which can be studied using different mucus stains (discussed later in this review).

3.1. Respiratory Tract *In Vitro* Cell Culture Models

There are a variety of transformed, cancerous, and primary bronchial epithelial cells that have been used to investigate drug and particle diffusion. A bronchial epithelial cell line, 16HBE14o-, was immortalized with Simian Vacuolating Virus (SV40) large T-antigen to obtain cells that proliferate indefinitely[91]. The 16HBE14o- cells have differentiated epithelial morphology and functional tight junctions, but do not secrete airway mucins MUC5AC or MUC2 [92]. Although 16HBE14o- can be cultured with or without liquid in the apical chamber, liquid culture was required for 16HBE14o- monolayers to express localized zonula-occludens-1, which is an essential tight junction protein[93]. The bronchial carcinoma cell line, Calu-3, is a mixture of both ciliated and secretory cells that secrete mucin (MUC5AC) at an air-liquid interface. Similar to 16HBE14o-, Calu-3 cells can be cultured by two different methods: submerged in fluid and at an air-liquid interface; where submerged cells have shorter and thicker cilia than cells cultured at the air interface[94]. After Calu-3 cells were cultured on cell culture inserts for 48 hours, an air-liquid interface was implemented, with media in the basolateral chamber and no liquid in the apical chamber[95]. Polarized monolayers with a TEER > 300 Ohms*cm^2 were used between day 8 and 16 of air-liquid interface culture for drug transport studies. Drug in Bicarbonate Ringer's Solution was added to the apical chamber and 100 μL of basolateral media was collected and analyzed for drug concentration for up to 3 hours. Permeability of drugs (e.g., propranolol, antipyrine) was correlated with lipophilicity, and transport rate of hydrophilic drugs (e.g., caffeine, hippuric acid, theophylline) was inversely related to molecular weight. Drug permeability through Calu-3 monolayers correlated well with apparent permeability (P_{APP}) values for primary cultured rabbit tracheal epithelial mucus secreting cells, and *in vivo* rat lung absorption experiments. Calu-3 cultures have also been utilized to study particle bioadhesion[96]. Microparticles (~2–4 μm diameter) composed of starch, alginate, chitosan, or Carbopol® 971P-NF were loaded with fluorescent bovine serum albumin (BSA). To investigate bioadhesivity, particles were applied to the apical culture surface and

washed after 0.5, 2, or 6 hours. Both alginate and starch microparticles were not adhesive after 0.5 hours, while chitosan and Carbopol® were both adhesive at 6 hours.

Unlike cell lines, primary airway epithelial cell cultures contain a heterogeneous cell population including ciliated, secretory, and basal cells that secrete tissue-specific mucins[97]. Primary human epithelial bronchial cells cultured on Transwell® developed cilia and secreted a mucus layer after 6 weeks of culture at an air-liquid interface[98]. Secreted mucus was collected and MPT was used to analyze the diffusion of carboxyl-modified polystyrene particles (1 μm in diameter) in mucus. Particle mobility decreased and the storage and elastic moduli increased as mucus solid wt% increased from 1.5 to 5. This work highlighted the importance in considering particle size, where particles larger than the mucus mean pore size do not undergo normal Brownian diffusion. In another study, normal human bronchial epithelial cells, commercially available from Lonza, were cultured at an air-liquid interface for 6 days and expressed MUC5AC mRNA and protein intracellularly[99, 100]. The transport of anti-allergic drugs in media (Hank's balanced salt solution buffered with 10 mM HEPES and 10 mM D-glucose) from the apical to the basolateral side was studied over 2 hours. Drug diffusion depended on the partition coefficient, where albuterol hemisulfate, a hydrophilic compound (logP = −1.58), and budesonide, a lipophilic compound (logP = 3.21), had P_{APP} values of 0.92 * 10^{-6} and 9.06 * 10^{-6} cm/s, respectively. In comparison, P_{APP} values for albuterol hemisulfate diffusion across monolayers grown from immortalized cell lines, 16HBE14o- and Calu-3, were 1.42 * 10^{-6} and 5.33 * 10^{-6} cm/s, respectively. The difference in P_{APP} values may be attributed to the different physiological properties (e.g., mucus production, cell membrane permeability, barrier provided by tight junctions) of the primary compared to the immortalized monolayers.

3.2. Intestinal Tract *In Vitro* Cell Culture Models

The human colorectal adenocarcinoma-derived Caco-2 cell line can produce monolayers of enterocyte-like cells that are commonly used to study intestinal drug absorption[90]. While Caco-2 have membrane-bound mucins (MUC1), they do not produce secreted mucins, such as MUC2 and MUC5AC, the main secreted gel-forming mucins in the GIT[101]. Thus, co-cultures of Caco-2 with mucus-producing cells, representing the mucus-secreting goblet cells of the intestine, are commonly utilized to capture the impact of the mucus barrier. Mucus producing cells include the human colon adenocarcinoma-derived cell lines, HT29, HT29-MTX, and HT29-FU[90, 102]. When cultured as a confluent monolayer, only a small proportion of HT29 cells (~5%) differentiate and secrete mucus[102]. When cultured with 10^{-6} M methotrexate, HT29 irreversibly differentiates into HT29-MTX, an immortalized cell line that is morphologically similar to goblet cells. Mucins secreted from HT29 have a lower sialic acid and higher sulfate content relative to those from HT29-MTX[102]. While the Caco-2/HT29-MTX co-culture model is frequently used to represent the epithelial and mucosal barrier of the GIT, HT29-MTX cells only secrete gastric mucins MUC5AC, rather than MUC2. HT29-FU cells were adapted with 10^{-5} M 5-fluorouracil and primarily secrete MUC2, which are the main intestinal mucins[103]. To obtain mature, polarized monolayers that are morphologically and functionally similar to the native epithelium, Caco-2 can be cultured with mucus-producing cells (i.e. HT29-MTX, HT29-FU) for 21 days. Caco-2/

HT29-MTX seeded at a 3:1 ratio had a mucus thickness of ~4 μm[104]. Thus, the mucus secreted in these *in vitro* cell cultures is significantly thinner than mucus layers found on human and mouse colonic explants (approximately 600 and 450 μm thick, respectively)[23].

To study the impact of the mucus layer on drug diffusion, (1) cultures containing mucus-producing cells (e.g., Caco-2/HT29 co-culture) can be compared to cultures where mucus-producing cells are omitted (e.g., Caco-2); (2) drugs can be used to stimulate mucus secretion, allowing comparison of the impact of different amounts of mucus; (3) the mucus layer can be removed by chemical methods from cultures in which mucus is produced; or (4) purified mucin can be added to a culture devoid of mucus-producing cells. Caco-2 and HT29 can be co-cultured at different ratios to increase the proportion of mucus-producing cells; however, TEER values can decrease with an increase in the concentration of HT29 mucus-secreting cells[105]. After 21 days of co-culture, Caco-2:HT29 at 1:0, 9:1, and 0:1 had TEER values of 300 ± 7.6, 263 ± 3.6, and 150 ± 3.6 Ohms*cm^2, respectively. The higher TEER value of Caco-2 mono-cultures compared to co-cultures may reflect differences in propensity for paracellular (i.e. passive transport through cell junctions) drug diffusion. Treating cell monolayers with N-[(3,5-Difluorophenyl)acetyl]-L-alanyl-2-phenyl]glycine-1,1-dimethylethyl ester (DAPT), a Notch γ-secretase inhibitor, promoted goblet cell differentiation and mucus production[106]. HT29-MTX-E12, a HT19-MTX sub-clone, had mucus layers 3–5 μm and 10–15 μm thick when cultured under standard culture conditions and in the presence of DAPT, respectively. N-acetyl cysteine (NAC), a mucolytic agent, cleaves disulfide bonds within the cross-linked mucus gel[62, 107], and thus has been used to remove the secreted mucus layer from cell cultures. A HT29-MTX E12 sub-clone monolayer can be exposed to 10 mM NAC in buffer for 1 hour at 37 °C to remove the mucus layer without affecting monolayer integrity. A 2-fold increase in the number of 200 nm polystyrene nanoparticles associated with a HT29-MTX E12 monolayer was observed after NAC removal of the mucus layer [108], indicating that the secreted mucus was a barrier to particle diffusion. Finally, mucin can be added to Caco-2 cultures, which do not secrete mucin, to obtain a mucus layer of specified thickness and composition. Sigma gastric mucin (40 mg/mL) added to Caco-2 monolayers 20 minutes prior to inoculation with *Escherichia coli* significantly inhibited bacterial translocation across the enterocyte monolayer[109].

Primary intestinal and gastric organoids can be cultured in growth factor-enriched media and differentiated to include epithelial cells, including goblet cells that stain positive for MUC2[110, 111]. Moreover, organoids grown in a 3D culture can develop morphological features similar to *in vivo* tissue, including crypt-like structures. Since the interior of the organoid represents the intestinal lumen, microinjection has been utilized to inject microbes, drugs or drug carriers into the lumen to study their interaction with the luminal (mucosal) surface[112]. Alternatively, intestinal organoids can be disrupted mechanically and/or enzymatically to partially “open” them and expose the mucosal surface to certain agents of interest. However, some concerns with these techniques include the low throughput and time associated with microinjection, and potential damage to organoids with microinjection and mechanical/enzymatic disruption. In addition, cultures of intestinal organoids can exhibit variability in organoid structure and differentiation state. Organoids can also be disassociated and seeded as a monolayer on cell culture insert membranes[113, 114]. Ileal and rectal monolayers had a mucus thickness of approximately 26 and 36 μm,

respectively[114], which is thinner than mucus layers *in vivo* (200–700 μm), but thicker than mucus layers on cell lines (<10 μm). Due to the limited number of studies on primary monolayers to date, they have not yet been well characterized with respect to differentiation state (e.g., number and function of goblet cells, Paneth cells, enterocytes, etc.) or their impact on drug or particulate diffusion.

3.3. Multi-organ Models

Recent advances in microfluidic platforms allow for the analysis of the cross-talk between different tissues, including mucosal tissues[92, 93]. In one on-chip organ model, airway and liver modules were composed of primary human bronchial epithelial cells and primary human hepatocytes, respectively[92]. The bronchial epithelial cells were cultured for 14 days at an air-liquid interface, resulting in barrier function (tight junction formation, cell polarity) and mucus secretion rates similar to those of *in vivo* airway epithelium. In another system, human liver (i.e. human primary hepatocytes and Kupffer cells) and intestinal (C2BBe1 Caco-2 clone, HT29-MTX, and human primary dendritic cells) modules were used to study gut-liver interaction for 2 weeks[115, 116]. Endotoxemia, a condition characterized by the presence of circulating lipopolysaccharide (LPS), was simulated by the addition of 2 ng/mL LPS into the circulating media. Analysis of secreted cytokines revealed non-linear modulation of responses (e.g., production of CXCR3 ligands) in the integrated system. A different microfluidic platform incorporated intestine, liver, skin and kidney modules[117]. EpiIntestinal™(MatTek Corporation), which is composed of enterocytes, Paneth cells, M cells, tuft cells, and intestinal stem cells, was incorporated as the intestine module. Glucose added to the apical media of the intestine module decreased 4-fold compared to dosed concentration. Organ-on-chip microfluidic platforms can ultimately be used to study drug diffusion across mucus and epithelial barriers in systems capturing effects of organ cross-talk.

4. Tissue and Animal Models to Investigate Mucosal Drug Delivery

While native collected mucus, purified mucin, and *in vitro* cell cultures can be used to significantly increase understanding of the role mucus plays in drug delivery; *ex vivo* and *in vivo* studies of the mucus layer on actual tissue more fully capture the composition, thickness, architecture, and dynamic nature of the native mucosal environment. Drugs and drug delivery systems can be introduced to the GIT (e.g., by oral administration, gastric gavage, injection into ileal loops, or intestinal perfusion), respiratory tract (e.g., by inhalation or intranasal/intratracheal administration), or vaginal tract (e.g., by intravaginal administration) before *ex vivo* or *in vivo* analysis[118]. *Ex vivo* and *in vivo* studies can be conducted on tissue from different anatomical sites for the investigation of site-specific drug diffusion and penetration through mucus and underlying epithelium. However, both *in vivo* and *ex vivo* studies are limited by tissue availability and can be prone to animal to animal variability.

4.1. Techniques to Analyze Mucus Thickness, Drug Absorption and Distribution on Excised Mucosal Tissue Samples

Tissue samples have been extracted from different animal models (e.g., lapine, murine, canine, ovine) and humans for analysis of mucosal barrier properties. These samples have been collected from several anatomical locations including the nasal mucosa[119, 120], trachea[121], stomach[122], intestine[123, 124], and colon[125]. Studies are often performed using animal models due to limited availability of human tissues. Human samples are mainly obtained during surgical procedures (e.g., corrective gastro-intestinal surgeries to resect diseased tissue or to reduce stomach volume); however, these diseased tissues likely have altered barrier properties[63, 126]. Human samples from the trachea and nasal mucosa are less readily available but can be obtained from transplant rejections[127], airway biopsies[128], fetal tissue[129], nasal septum surgery[130], or nasal turbinate removal[131].

Diffusion studies on excised tissue have included analysis of particle diffusion with MPT[63, 132], particle penetration through intact mucus on tissue by confocal microscopy[133–135], and molecular transport across mucus and underlying tissue using fluorescence spectrophotometry[136–138]. As with *in vitro* cell cultures, one challenge of conducting MPT on excised tissue specimens is ensuring that the particles being analyzed are within the mucus layer, which could be 10–800 μm thick depending on animal and tissue source. If the tissue is submerged in a solution, it may be difficult to ensure particles are within the mucus rather than above the mucus layer or in underlying cells. This can be further complicated due to complex tissue architecture, such as crypt-villus architecture present in the intestine, where the mucus layer does not comprise an even, flat layer but rather a gel coating a complex, irregular shape. To ensure particles are tracked in mucus, tissue topography can be visualized with fluorescence microscopy and particles can be added in small volumes utilizing capillary flow to negate tracking particles in areas of excess dosed solution. MPT technique was used to show there was no statistical difference between transport of 100 nm carboxylate-modified and PEGylated polystyrene particles on native collected mouse mucus and excised mouse tissue with an intact mucus layer[132]. Particle diffusion rates were found to be greater in mucus on excised small intestine relative to trachea, colon, and vagina[132]. Differences in transport properties with anatomical position may be due to variations in mucus structure (e.g., pore size), composition, and thickness. For example, predicted pore size based on MPT analysis and the obstruction scaling model was 340 ± 70 nm in cervicovaginal mucus, and 150 ± 50 nm in human nasal mucus collected from patients with chronic rhinosinusitis, an inflammatory condition of the sinuses[139].

Intestinal mucosal permeability to fluorescein isothiocyanate (FITC)-dextran, a commonly used and biologically inert permeability marker, was studied using excised intestinal loops. The intestine was sutured at one end, injected with FITC-dextran, sutured at the other end, and incubated in buffer. At different times, buffer samples were collected, and fluorescence was measured to calculate mucosal permeability over a 6 hour time period[140]. This method was used to demonstrate a ~40-fold increase in permeability across the small intestine of rats with sodium deoxycholate-induced pancreatitis. It is noted that “mucosal transport” or “mucosal permeability,” as noted here, is often used to refer to permeability across the mucus layer together with underlying epithelium. Similar to *in vitro* cell culture

permeability studies, drug transport through mucus in *in vivo* and *ex vivo* samples is difficult to study in isolation, as drug can partition into the underlying epithelium. Indeed, in this last example, the permeability reflects the barrier properties of the mucus and underlying epithelium, as well as the underlying mesenchymal and muscular layers of the intestinal wall. Everted gut sac experiments are similar to intestinal loops, except that the excised intestinal segment is everted, sutured at both ends, and incubated in a buffer solution containing a drug or drug carrier. After the desired length of time, the tissue is opened and the fluorescence of the internal solution is analyzed[136–138]. This everted gut sac configuration was used to show that FITC-dextran transport across jejunum tissue increased in the presence of ac-A_6D-COOH lipid-like peptides, indicating these lipid-like peptides increase the permeability of the jejunum[138]. Intestinal permeability after ischemia was measured on tissue using the everted gut sac model with and without removal of the mucus layer. Treatment with 10% NAC to remove mucus significantly increased FITC-dextran permeability in ischemia samples ~2.5-fold as compared to ischemia samples without NAC treatment[137], indicating the mucus layer plays a crucial role in intestinal permeability. While both techniques described above allow the investigation of permeability through tissue, the everted gut model may alter the barrier due to stretching of tissue and possible removal of mucus during the process of inversion.

Ussing chambers have been used to extend *ex vivo* tissue viability for up to 2.5 hours[141–143], as they enable mixing and thus improved mass transport between tissue and surrounding medium. Similar to a cell culture insert setup, an Ussing chamber system consists of a donor and acceptor compartment separated by the tissue sample, with the entire apparatus enclosed in a temperature controlled water jacket. Both donor and acceptor chambers are filled with buffer (e.g., Krebs-Ringer bicarbonate buffer) through which gas (e.g., carbogen gas: 30% carbon dioxide, 70% oxygen) is bubbled to oxygenate the system and facilitate mixing. This experimental apparatus can be used to monitor tissue permeability, and since it enables mixing, can be used to examine simultaneous drug dissolution and permeation. Ussing chambers can have a horizontal or a vertical configuration (Fig. 4B and 4C). The vertical Ussing chamber setup can be used to investigate transport through a liquid-liquid interface, while the horizontal diffusion chamber can incorporate an air interface, for example, as present in the respiratory tract. In addition to increased tissue viability compared to static *ex vivo* tissue explant cultures, benefits of the Ussing chamber setup include the ability to test more conditions (e.g., drugs) per animal compared to *in vivo* experiments. However, Ussing chambers incorporating *ex vivo* tissue samples can be limited by low throughput (as compared to experiments utilizing *in vitro* cell cultures or isolated mucus specimens), and tissue variability, and limited tissue viability past 2.5 hours, in part due to lack of capillary circulation. In a study with 25 different drugs, both drug physicochemical properties and anatomical location affected permeability through excised human tissue in Ussing chambers. For example, ximelagatran had the highest and lowest permeability in duodenum and ileum, respectively; while atenolol had the highest and lowest permeability in jejunum and colon, respectively[143].

Tissue permeability measured *ex vivo* using Ussing chambers can be compared to Caco-2 permeability measured in static (cell culture insert) as well as dynamic (Ussing chamber) cultures. Net transport rates of ceftibuten, a Biopharmaceutics Classification System (BCS)

class 2 (high permeability, low solubility) drug, and mannitol across intestinal tissue were faster than those measured across static Caco-2 cultures in cell culture inserts[144]. Similarly, permeability of PEG was greater in rat ileum than in rat colon, and lowest through Caco-2 cells[145]. Permeabilities of angiotensin II inhibitors through rat duodenum, jejunum, ileum, and colon mounted in Ussing chambers were different from each other, but all higher than through static Caco-2 cultures[146]. When cell cultures and tissues were both mounted in Ussing chambers, permeation of clarithromycin, another BCS class 2 drug, was greater through Caco-2 cell cultures compared to excised rat intestinal tissue, potentially due to the additional release of mucus post-harvest[147]. Permeabilities across both the cell cultures and *ex vivo* tissue were greater than those measured *in vivo*[147].

Fluorescence and bright field microscopy have been used in conjunction with the Ussing chamber setup to investigate mucus thickness and barrier properties. Specifically, a suspension of fluorescent beads or charcoal particles is applied to the mucus surface and imaged or probed with micropipette and micromanipulator to determine mucus thickness of tissue mounted in an Ussing chamber. A suspension of charcoal particles on excised intestinal segments revealed *Citrobacter rodentium* infection altered mucus thickness over the course of infection. Tissue samples were removed and analyzed at different time points (days 0, 4, 10, 14, 19) after oral dosing of *Citrobacter rodentium*. Mucus thickness declined on day 4, followed by a significant increase on day 14[148]. During infection, mucin transcription and mucus secretion were altered, resulting in a change in mucus thickness[148]. The horizontal Ussing chamber setup has also been used to study the altered mucosal barrier in diseased tissue (e.g., ulcerative colitis (UC)) compared to healthy tissue. A particle suspension containing 200 and 500 nm fluorescent polystyrene particles was added on top of the mucosal surface of tissue from healthy and UC patients, incubated for 40 minutes to allow particles to diffuse, and imaged using a fluorescence microscope. Particles that penetrated the mucus layer and were located within 120 μm of the epithelial layer were classified as close to the epithelium. Excised samples from healthy patients had 0% of beads close to epithelium, while UC patients in remission had 10% and active UC had ~40% of beads close to the epithelium (Fig. 5)[134]. In contrast, CF, which is characterized by mucus hypersecretion, had an opposite effect on particle transport. Specifically, 2 μm beads added to small intestinal mouse tissue were able to penetrate control mucus but unable to penetrate CF mucus[133].

4.2. Analysis of Absorption and Distribution After *In Vivo* Administration

After administration at a mucosal site, drugs and drug carriers are exposed to physiological stimuli (e.g., microbial, immunological, hormonal) and must overcome mucus secretion, clearance and binding interactions to penetrate the epithelium. A number of different techniques can be employed to examine the distribution of dosed drug or drug carrier after administration *in vivo*. Often, serum drug concentration levels are analyzed. In these analyses, the isolation of the role of mucus is again complicated, as drug must also be transported across the epithelial barrier, and into the capillaries, before being detected in the blood. For example, intestinal permeability was investigated *in vivo* by measuring fluorescence of an orally dosed FITC-labeled marker in serum at different times. Orally ingested chlorpyrifos (a pesticide) statistically increased intestinal permeability, with the

FITC-dextran marker appearing in serum samples after 330 minutes, but not in control animal serum throughout the 400 minute experimental time period[149].

Intestinal perfusion or closed loops[150–152] can also be used to explore mucosal permeability. In intestinal perfusion studies, a segment of intestine is exposed, and each end of the segment is cannulated[153]. The segment is then returned to the intestine, flushed with phosphate buffered saline, and drug or drug carrier solution is infused into the segment. Collected intestinal perfusate and blood samples are then analyzed for drug content by an appropriate technique (e.g., high-performance liquid chromatography). Absorption of fenofibrate powder suspensions and nano-suspensions was investigated in the duodenum, jejunum, ileum and colon. Anatomical position and form of suspension affected absorption as indicated by concentration of drug in the perfusate; absorption of powder suspensions was greatest in the ileum (63%) and lowest in the jejunum (49%) while absorption of nano-suspensions was highest in the ileum (78%) and lowest in the colon (76%)[151]. In another study, an intestinal jejunum cannula was used to dose FITC-dextran in oil suspension (OS) or saline solution to study the effect of OS on intestinal mucosal permeability in rats. After 90 minutes, there was a significant increase in FITC-dextran marker in plasma samples following OS administration relative to saline administration[150]. In intestinal loops, a segment of intestine is exposed, sutured at both ends and injected with drug or particles, after which the intestine can be placed back in the abdomen and incubated for a desired length of time. The segment can then be excised and prepped for confocal microscopy or histological analysis[152]. One hour post-injection, M cell-homing peptide ligand-immobilized chitosan nanoparticles (CKS9-CNs) were localized in M cells, compared to un-localized CNs without immobilized peptide ligands. One limitation of perfusion and closed loop technique is that infusion and injection into the intestine do not recapitulate the effects of normal gut mobility and flow of lumen contents.

Drug or drug carrier distribution can be directly visualized *in vivo* (e.g., via magnetic resonance imaging (MRI) or an in vivo Imaging System (IVIS®)[154–156]), or after tissue is externalized (e.g., via two-photon microscopy (TPM)[154–160]) or excised and straightened for ease of visualization (IVIS®)[154, 158]. After intravaginal administration, liposomes (7 mol% PEG) loaded with barbituric acid (BA) were monitored by diamagnetic chemical exchange saturation transfer MRI. Liposomes loaded with BA were retained longer than 90 minutes and were evenly distributed throughout the vaginal tract, while unencapsulated BA was retained for ~30 minutes and accumulated in clusters[154]. IVIS® analysis 6 hours after intravaginal administration indicated PEGylated particle fluorescence was steady, while the fluorescence of carboxylate-modified particles decreased to 10% of initial values, suggesting carboxylate-modified particles were being cleared from the vaginal tract[155]. IVIS® was also used to monitor orally administered fluorescent *Bacteroides fragillis* (*B. fragilis*) temporal-spatial distribution in the GIT[158]. Overall fluorescence decreased with time, but was still detectible after 96 hours. Imaging via IVIS® and MRI are limited by the requirement of drugs or drug carriers to be labeled with a fluorescent marker or MRI contrast agent, respectively. Moreover, fluorescence microscopy is only able to image at limited depths of tissue due to light scattering[161]. Thus tracking of single particles as preformed on *ex vivo* tissue and/or collected mucus is not possible with these techniques.

To overcome limitations of *in vivo* imaging, tissues of interest (e.g., intestine) may be externalized (i.e. taken outside the body while leaving connected to surrounding tissue). To minimize tissue movement (e.g., peristalsis) when imaging, tissue can be immobilized by tissue adhesive in a humid glass imaging window. This set-up is able to maintain tissue viability for a relatively long period of time (~3 hours) [159]. Following intragastric dosing of *Vibrio chlorea*, TPM was used to visualize distribution and penetration into intestinal crypts through the wall of the intestine, without exposure of the luminal surface [157]. TPM uses nonlinear optical microscopy techniques to increase focal depth, allowing for the visualization of fluorescent components through tissues at depths up to 1.6 mm[160, 162]. In another study, fluorescent *B. fragillis* was administered by oral gavage or injected directly into the intestinal segment, and distribution on exposed intestinal lumen was imaged after 6 hours by TPM[158].

The native 3D architecture of tissue (e.g., intestinal crypts and villi, intertwining of the intestine), and overlapping organs can complicate the imaging of drugs and drug carriers *in vivo*. Tissue excision followed by straightening or flattening can be used to clarify drug dispersion. After oral dosage of fluorescent *B. fragilis*, the GIT was excised and straightened at multiple time points to enable direct visualization of microbe position and movement over time. The highest fluorescence intensity was initially observed in the stomach and mid-intestine (2 hours), followed by ileum and cecum (6 hours), and finally in cecum and colon (12 hours)[158]. After intravaginal injection, excised tissue was opened and flattened between two coverglass slides to reveal that uncoated liposomes (0 mol% PEG) were mucoadhesive and had non-uniform dispersion with areas of aggregation on the vaginal mucosa, while liposomes with 3 and 7 mol% PEG had increased dispersion and decreased aggregation [154]. Similarly, in another study, PEGylated and carboxylate-modified particles were distributed across 88% and 33% of the vaginal tissue, respectively[163].

4.3. Animal Models with Altered Mucus Barriers

Animal models can be highly useful for investigating the role of an altered mucus barrier in drug delivery, as well as the role it may play in disease or interactions with the microbiome. Animal models with altered mucus barriers include germ free and gene knockout animal models, as well animal models of specific disease states.

4.3.1. Germ Free vs. Wild Type Models—In recent years, interest in and studies focused on understanding the role of the microbiome in health and disease have dramatically increased[164–169]. While mucus controls diffusion of drugs and drug carriers to epithelium, it also plays the critical role of modulating interactions between the microbiome and underlying tissues. Germ free animals have been important for enabling studies of the impact of the microbiome, and their mucus barriers differ significantly from those of wild type animals. Germ free mice have altered mucin glycosylation[170] and expression[171–173]; increased mucin carbohydrate concentration[174]; and decreased adherent mucus layer thickness[175, 176] and number of mucus-producing goblet cells[173], relative to wild type mice. Ileum and colon mucin expression (Muc1, Muc2, Muc3, Muc4) were restored to normal levels with the introduction of a murine microbiome, indicating the presence of the microbiome alters the mucus barrier by degrading mucin and stimulating mucin

secretion[174–176]. Human microbiome samples can also be introduced to germ free mice to make the model more relevant to human studies, however, application of human microbiome to a murine model did not restore ileum and colon mucin expression (Muc1, Muc2, Muc3, Muc4) to normal levels reported in wild type mice[171].

4.3.2. Mucin Knockout Models—Knockout (KO) animal models can be used to investigate the significance of specific mucins in mucosal barriers and the associated impact on drug delivery and absorption. Currently, there exist six mucus knockout/null animal models for: Muc1[176–188], Muc2[189–194], Muc5[193, 195–197], Muc13[185, 198], Muc16[199–201], and Muc18[202–204]. Besides mucin KO models, alternative KO models are available to further elucidate the role of mucin glycosylation[205, 206] and other mucus components (e.g., growth factors[207]) on mucus barrier properties.

Mucin KO mice were similar to wild type mice with respect to viability[178, 198, 199], development[198, 199, 208], fertility[178, 199, 208], and weight[190]. However, Muc KO animal models have other abnormalities (Table 2), primarily displaying increased levels of colitis and inflammation[191, 192, 198, 209] or changes in other Muc gene expressions[195–197]. *Muc KO models have been used to investigate the role of specific mucins in bacterial penetration and colonization of the mucosa* [180, 193]*, inflammatory response to pathogen exposure*[180, 181, 185, 189, 193, 204], susceptibility to inflammation[176, 184–186], cancer and tumor formation[177–179, 190, 200], and rate of wound healing[182, 183, 201]. To measure intestinal uptake in Muc1 KO and wild type mice, [^{14}C]cholesterol and [^{3}H]palmitic acid were injected into the cannulated duodenum[187]. After 45 minutes, the intestine was harvested and radioactivity was measured, showing that intestinal absorption of cholesterol was reduced 50% in Muc1 KO compared to wild type mice, while palmitic acid absorption was not impacted.

4.3.3. Animal Models of Disease—Diseases associated with inflammation, including cystic fibrosis (CF), Hirschsprung's disease (HD), and ulcerative colitis (UC), can be associated with alterations in the mucus barrier[210, 211]. CF is caused by a mutation in the CF transmembrane regulator (CFTR) gene, resulting in mucus overproduction and chronic inflammation[212, 213]. CFTR$^{-/-}$ KO animals have increased secretion of Muc1, number of goblet cells and intestinal crypts filled with mucus, and deaths due to gastrointestinal obstruction[214]. In a CFTR$^{-/-}$ mouse model, about 10% of newborn mice had a meconium ileus, or stool blockage of the bowel, and after 30 days, 85% of the CFTR$^{-/-}$ mouse pups died and had distended crypts, increased mucus amounts, and destroyed intestinal villi. Due to the short lifespan of CFTR$^{-/-}$ KO mice, they do not develop symptoms of CF, and thus cannot be utilized to study CF in the respiratory tract. Therefore, to study CF, a mouse model with S489× mutation of the CFTR gene was developed and challenged with *Pseudomonas aeruginosa*[215]. After 10 days of microbe exposure, adult mice showed signs of significant pulmonary inflammation and increased cytokine expression compared to normal mice.

Another disease associated with intestinal inflammation, HD, is a condition that affects the large intestine and is characterized by the improper development of nerve cells, absence of bowel movement, bacterial infection of intestinal tissue, and abdomen distension[216]. To

explore potential changes in colonic mucus barrier properties associated with HD, the colon was extracted from a murine HD model (11–20 day old Endothelin receptor B mutant ($Ednrb^{-/-}$)) or wild type mice, and particle movement on tissue was analyzed using MPT. The average diffusion rate of 200 nm carboxylate-modified particles was decreased 1.5-fold in distal colonic mucus and ~7-fold in proximal colonic mucus of HD mice relative to wild type. Interestingly, while HD primarily affects the distal colon, an altered mucus barrier was also observed in the proximal colon[63].

Oral administration of dextran sodium sulphate (DSS) to rats and mice results in intestinal injury with features similar to human UC, a chronic inflammatory disease of the colon. Oral DSS dosing increased epithelial permeability, decreased mucus layer thickness, and upregulated chemokine and cytokine expression[217, 218]. Colitis severity was dependent on DSS concentration, molecular weight, length of exposure, and animal model strain, gender, and microbiome composition[210, 211]. After introduction of 4% DSS in chow of Wistar rats for 5 days, the distal colon was isolated for mannitol permeability studies using the Ussing chamber setup[219]. The DSS exposed tissue had higher mannitol permeability compared to control tissue. Interestingly, when butyrate, a short chain fatty acid, was added to the mucosal side in the Ussing chamber, mannitol permeability decreased through DSS exposed tissue, but was still higher compared to control.

5. Fixation and Characterization of Mucus Layer

As noted above, mucosal tissue samples can be fixed or frozen for structural and histological analysis to facilitate investigation of particle penetration and distribution and/or the impact of drug or drug carrier on mucus properties (e.g., structure, thickness). However, proper fixation is challenging and prone to artifacts due to the high concentration of water (~97%) present in mucus and the highly-glycosylated nature of mucin molecules. Tissue samples are commonly preserved in Karnovsky's or formalin fixative, but these fixation techniques can result in collapse and/or removal of the mucus layer[220–222]. Thus, less common non-aqueous fixatives, including Carnoy's fixative[134, 222], acetone[223], and tetradecafluorohexane[221], have been reported to better preserve the mucus layer during fixation. Some protocols may include a post-fixation step with osmium tetroxide to further preserve the mucus layer before embedding in paraffin wax or epoxy resin and sectioning. These non-aqueous fixatives may aid in maintaining the mucus structure by different mechanisms, e.g., minimizing water movement out of the gel or mitigating surface tension effects[221]. Cryopreservation can also be utilized to preserve the mucus layer[224], and has been used to enable visualization of mucus thickness[225], mucus proteins[226], goblet cells[227], and particle distribution[228]. Non-fixed and fixed mucosal tissue samples may be embedded in optimal cutting temperature (OCT) compound, snap frozen in isopentane cooled with liquid nitrogen, and then sectioned. Non-chemically fixed tissue sections may then be fixed with 10% formalin to prevent tissue degradation[229]. One method to preserve tissue structure before embedding involves rapid freeze and freeze substitution[230]. Briefly, samples are plunge frozen in Freon™ or liquid nitrogen and then fixed with osmium tetroxide dissolved in acetone[223]. Tissue samples are then be embedded in epoxy resin, thin sectioned, and analyzed by electron microcopy. A major limitation of cryopreservation methods are freezing artifacts from the crystallization of water resulting in cellular

disruption and polymer-induced compression of mucus by the embedding medium[231]. Other techniques have also been utilized to preserve and visualize the mucus layer (e.g., cryo- or environmental scanning electron microscopy[232, 233]). Overall, proper fixation to preserve structure and visualization of the mucus layer at high resolution remains a significant challenge.

Various staining and labeling techniques are used to allow visualization of goblet cell depletion[234], mucin distribution, thickness, and glycosylation[148, 235], and particle distribution within mucus. Negatively-charged mucins can be visualized with positively-charged Alcian blue stain[105], and neutral mucins and polysaccharides can be stained with Periodic acid-Schiff[106]. Specific mucins (e.g., MUC1, MUC2, MUC5ac, MUC6, and MUC13), can also be identified using antibodies[106]. Mucin sugars can be visualized using fluorescently-tagged lectins: wheat-germ agglutinin binds terminal N-acetyl-D-glucosamine and sialic acid[157], *Ulex europaeus* agglutinin-1 binds L-fucose[236], con-canavalin A binds α-mannose and α-glucose[237], peanut agglutinin binds galactose[238], and *Dolichos biflorus* agglutinin binds N-acetylgalactosamine[238]. Additionally, fluorescent *in situ* hybridization (FISH) can be used to identify bacterial DNA and proximity to the epithelium.

Comparison of paraffin-embedded Carnoy's-fixed sections from colonoscopy samples immunostained for MUC2 demonstrated that the mucus layers from healthy individuals orally dosed with or without laxatives were significantly thicker than the mucus layers from individuals with UC[134]. After rats were orally dosed with soybean oil or phosphate buffered saline, paraffin-embedded Carnoy's-fixed sections stained with lectin and Hoescht® showed the ingestion of soybean oil reduced penetration of 200 nm carboxylate-modified nanoparticles[59]. In another study, cryosections of vaginal epithelium stained with 4,6-Diamidino-2-phenylindole (DAPI) revealed that carboxylate-modified particles dosed in a hypotonic solution aggregated in the vaginal lumen, while PEGylated particles formed a continuous layer coating the entire vaginal epithelium within 10 minutes of intravaginal injection[155]. Cryosections of lung tissue stained with DAPI indicated similar results when PEGylated particles were administered. Briefly, mice were intranasally administered Cy3-labeled gene carriers and lungs were harvested after 2 hours. PEGylated-polyethylenimine particles (56 nm) were uniformly dispersed at the mucosal surface, with 70% retained over 6 hours, while uncoated-polyethylenimine particles (52 nm) were aggregated, with only 30% retention after 2 hours[156].

6. Summary

In summary, mucus models have been used to study the significance of mucus and the mucosal barrier in drug delivery (e.g., drug and drug carrier adhesion, diffusion, penetration, absorption, and distribution). The properties of the mucus barrier (e.g., composition, structure, thickness) in these models, which can impact drug delivery, depend on mucus source, animal species, age, and disease. The ideal mucus model should recapitulate the composition and structure of native human mucus to the greatest extent possible; however, the selection of a model system may also be guided by ease of use, reproducibility, and ability to obtain specific measurements. Analyses conducted using native collected mucus and purified mucin preparations, which can include bulk and micro-rheology, MPT, and

measurements of mucin-drug interactions, inherently treat mucus as an isotropic medium. *In vitro* cell culture models incorporating mucus-producing cells can be used to measure absorption and penetration across the mucus layer in tandem with the underlying epithelial layer, which acts as another barrier to drug diffusion; however, cell-secreted mucus layers *in vitro* are typically significantly thinner than those present *in vivo* (~10–40 μm vs. 100–700 μm, respectively). *Ex vivo* tissue samples provide a snapshot of the *in vivo* environment (e.g., mucus structure and composition) and aid in investigating mucus thickness as well as drug penetration and absorption. Drug and drug carriers can be administered *in vivo*, such that they are exposed to representative physiological conditions, including the dynamic mucosal barrier. However, limited optical resolution hinders *in vivo* imaging of drug and drug carriers, and *in vivo* analyses are thus generally limited to monitoring of overall absorption or macroscopic distribution, although advanced microscopic analyses (e.g., intravital TPM) or extraction of tissue samples for analysis *ex vivo* can aid in overcoming this barrier. Thus, it is crucial to consider the advantages and disadvantages of the various models when selecting a model system to investigate the role of the mucus barrier in drug delivery.

Funding:

This work was supported by the March of Dimes (MoD #6-FY14–404); National Institutes of Health (NIH 1RO1EB021908–01); Northeastern University Dissertation Completion Fellowship; and U.S. National Science Foundation Graduate Research Fellowship Program for supporting Jaclyn Lock (GRFP 2012125281).

References

[1]. Dekker J, Van Beurden-Lamers WM, Oprins A, Strous GJ, Isolation and structural analysis of rat gastric mucus glycoprotein suggests a homogeneous protein backbone, The Biochemical Journal 260(3) (1989) 717–723. [PubMed: 2764900]

[2]. Larsson J, Karlsson H, Sjovall H, Hansson G, A complex, but uniform O-glycosylation of the human MUC2 mucin from colonic biopsies analyzed by nanoLC/MSn, Glycobiology 19(12) (2009) 1568–1569.

[3]. Lai SK, O'Hanlon DE, Harrold S, Man ST, Wang YY, Cone R, Hanes J, Rapid transport of large polymeric nanoparticles in fresh undiluted human mucus, Proceedings of the National Academy of Sciences of the United States of America 104(5) (2007) 1482–1487. [PubMed: 17244708]

[4]. Suk JS, Lai SK, Wang Y-Y, Ensign LM, Zeitlin PL, Boyle MP, Hanes J, The penetration of fresh undiluted sputum expectorated by cystic fibrosis patients by non-adhesive polymer nanoparticles, Biomaterials 30(13) (2009) 2591–2597. [PubMed: 19176245]

[5]. Witten J, Ribbeck K, The particle in the spider's web: transport through biological hydrogels, Nanoscale 9(24) (2017) 8080–8095. [PubMed: 28580973]

[6]. Lehr C-M, Poelma FGJ, Junginger HE, Tukker JJ, An estimate of turnover time of intestinal mucus gel layer in the rat in situ loop, International Journal of Pharmaceutics 70(3) (1991) 235–240.

[7]. Corbo GM, Foresi A, Bonfitto P, Mugnano A, Agabiti N, Cole PJ, Measurement of nasal mucociliary clearance, Archives of Disease in Childhood 64(4) (1989) 546–550. [PubMed: 2751328]

[8]. Bansil R, Celli JP, Hardcastle JM, Turner BS, The Influence of Mucus Microstructure and Rheology in Helicobacter pylori Infection, Frontiers in Immunology (2013).

[9]. Cone R, Mucus, in: Mestecky J (Ed.), Mucosal Immunology, Elsevier Academic Press, Amsterdam, 2005, pp. 49–72.

[10]. Hills BA, Gastric surfactant and the hydrophobic mucosal barrier, Gut 39(5) (1996) 621. [PubMed: 9026472]

[11]. Knowles MR, Boucher RC, Mucus clearance as a primary innate defense mechanism for mammalian airways, The Journal of Clinical Investigation 109(5) (2002) 571–577. [PubMed: 11877463]

[12]. Atuma C, Strugala V, Allen A, Holm L, The adherent gastrointestinal mucus gel layer: thickness and physical state in vivo, American Journal of Physiology - Gastrointestinal and Liver Physiology 280(5) (2001) G922. [PubMed: 11292601]

[13]. Johansson ME, Phillipson M, Petersson J, Velcich A, Holm L, Hansson GC, The inner of the two Muc2 mucin-dependent mucus layers in colon is devoid of bacteria, Proc Natl Acad Sci U S A 105(39) (2008) 15064–9. [PubMed: 18806221]

[14]. Katz DF, Slade DA, Nakajima ST, Analysis of pre-ovulatory changes in cervical mucus hydration and sperm penetrability, Advances in Contraception 13(2) (1997) 143–151. [PubMed: 9288332]

[15]. Emily Krogstad MR, Kim Woodrow, Vaginal Drug Delivery, in: Abraham Domb WK (Ed.), Focal Controlled Drug Delivery, Springer Science & Business Media 2014.

[16]. Litt M, Khan MA, Wolf DP, Mucus rheology: relation to structure and function, Biorheology 13 (1976) 37–48. [PubMed: 938740]

[17]. Sakata T, Engelhardt W, Luminal mucin in the large intestine of mice, rats and guinea pigs, Cell and Tissue Research 219(3) (1981) 629–635. [PubMed: 7273117]

[18]. Kararli TT, Comparison of the gastrointestinal anatomy, physiology, and biochemistry of humans and commonly used laboratory animals, Biopharmaceutics & Drug Disposition 16 (1995) 351–380. [PubMed: 8527686]

[19]. Karlsson NG, Herrmann A, Karlsson H, Johansson ME, Carlstedt I, Hansson GC, The glycosylation of rat intestinal Muc2 mucin varies between rat strains and the small and large intestine. A study of O-linked oligosaccharides by a mass spectrometric approach, The Journal of Biological Chemistry 272(43) (1997) 27025–27034. [PubMed: 9341141]

[20]. Freire AC, Basit AW, Choudhary R, Piong CW, Merchant HA, Does sex matter? The influence of gender on gastrointestinal physiology and drug delivery, International Journal of Pharmaceutics 415(1) (2011) 15–28. [PubMed: 21640175]

[21]. Van Der Waaij LA, Harmsen HJM, Madjipour M, Kroese FGM, Zwiers M, Van Dullemen HM, De Boer NK, Welling GW, Jansen PLM, Bacterial population analysis of human colon and terminal ileum biopsies with 16S rRNA-based fluorescent probes: Commensal bacteria live in suspension and have no direct contact with epithelial cells, Inflammatory Bowel Diseases 11(10) (2005) 865–871. [PubMed: 16189415]

[22]. Varum FJO, Veiga F, Sousa JS, Basit AW, Mucus thickness in the gastrointestinal tract of laboratory animals, Journal of Pharmacy and Pharmacology 64(2) (2012) 218–227. [PubMed: 22221097]

[23]. Gustafsson JK, Ermund A, Johansson MEV, Schütte A, Hansson GC, Sjövall H, An ex vivo method for studying mucus formation, properties, and thickness in human colonic biopsies and mouse small and large intestinal explants, American Journal of Physiology - Gastrointestinal and Liver Physiology 302(4) (2012) G430. [PubMed: 22159279]

[24]. Holmén Larsson JM, Thomsson KA, Rodríguez-Piñeiro AM, Karlsson H, Hansson GC, Studies of mucus in mouse stomach, small intestine, and colon. III. Gastrointestinal Muc5ac and Muc2 mucin O-glycan patterns reveal a regiospecific distribution, American Journal of Physiology - Gastrointestinal and Liver Physiology 305(5) (2013) G357. [PubMed: 23832516]

[25]. Moghissi KS SF, Cyclic changes in the amount and sialic acid of cervical mucus, International Journal of Fertility 21 (1976) 246–50.

[26]. Wolf DP, Sokoloski J, Khan MA, Litt M, Human cervical mucus. III. Isolation and characterization of rheologically active mucin, Fertility and Sterility 28(1) (1977) 53–58. [PubMed: 832716]

[27]. Iacobelli S, Garcea N, Angeloni C, Biochemistry of cervical mucus: A comparative analysis of the secretion from preovulatory, postovulatory, and pregnancy periods, Fertility and Sterility 22(11) (1971) 727–734. [PubMed: 5123248]

[28]. Lieleg O, Vladescu I, Ribbeck K, Characterization of particle translocation through mucin hydrogels, Biophysical Journal 98(9) (2010) 1782–1789. [PubMed: 20441741]

[29]. Tabata M, Tomomasa T, Itoh K, Miyashita M, Hyman PE, Tanaka T, Kuroume T, Developmental changes in gastric mucus gel thickness: responsiveness to 16,16-dimethyl prostaglandin E2 and mucosal protection in the rat, Pediatric Research 31(2) (1992) 193–195. [PubMed: 1542551]

[30]. Shub MD, Pang KY, Swann DA, Walker WA, Age-related changes in chemical composition and physical properties of mucus glycoproteins from rat small intestine, The Biochemical Journal 215(2) (1983) 405–411. [PubMed: 6651768]

[31]. Turck D, Feste AS, Lifschitz CH, Age and diet affect the composition of porcine colonic mucins, Pediatric Research 33(6) (1993) 564–567. [PubMed: 8378112]

[32]. Masaro L, Zhu XX, Physical models of diffusion for polymer solutions, gels and solids, Progress in Polymer Science 24(5) (1999) 731–775.

[33]. Peppas NA, Khare AR, Preparation, structure and diffusional behavior of hydrogels in controlled release, Advanced drug delivery reviews 11(1) (1993) 1–35.

[34]. Muhr AH, Blanshard JMV, Diffusion in gels, Polymer 23(7) (1982) 1012–1026.

[35]. Tokita M, Transport phenomena in gel, Gels 2(2) (2016) 17.

[36]. Cu Y, Saltzman WM, Mathematical modeling of molecular diffusion through mucus, Advanced drug delivery reviews 61(2) (2009) 101–114. [PubMed: 19135488]

[37]. Lai SK, Wang YY, Wirtz D, Hanes J, Micro- and macrorheology of mucus, Advanced drug delivery reviews 61(2) (2009) 86–100. [PubMed: 19166889]

[38]. Crater JS, Carrier RL, Barrier properties of gastrointestinal mucus to nanoparticle transport, Macromolecular Bioscience 10(12) (2010) 1473–1483. [PubMed: 20857389]

[39]. Rubin BK, Ramirez O, Zayas JG, Finegan B, King M, Collection and analysis of respiratory mucus from subjects without lung disease, The American Review of Respiratory Disease 141(4 Pt 1) (1990) 1040–1043. [PubMed: 2327638]

[40]. Schuster BS, Suk JS, Woodworth GF, Hanes J, Nanoparticle diffusion in respiratory mucus from humans without lung disease, Biomaterials 34(13) (2013) 3439–3446. [PubMed: 23384790]

[41]. Wolf DP, Blasco L, Khan MA, Litt M, Human cervical mucus. I. Rheologic characteristics, Fertility and Sterility 28(1) (1977) 41–46. [PubMed: 556703]

[42]. Boskey ER, Moench TR, Hees PS, Cone RA, A self-sampling method to obtain large volumes of undiluted cervicovaginal secretions, Sexually Transmitted Diseases 30(2) (2003) 107–109. [PubMed: 12567165]

[43]. Sanders NN, De Smedt SC, Van Rompaey E, Simoens P, De Baets F, Demeester J, Cystic fibrosis sputum: a barrier to the transport of nanospheres, American Journal of Respiratory and Critical Care Medicine 162(5) (2000) 1905–1911. [PubMed: 11069833]

[44]. Larhed AW, Artursson P, Gråsjö J, Björk E, Diffusion of drugs in native and purified gastrointestinal mucus, Journal of Pharmaceutical Sciences 86(6) (1997) 660–665. [PubMed: 9188047]

[45]. Smith GW, Wiggins PM, Lee SP, Tasman-Jones C, Diffusion of butyrate through pig colonic mucus in vitro, Clinical Science 70(3) (1986) 271–276. [PubMed: 3948476]

[46]. Crocker JC, Grier DG, Methods of digital video microscopy for colloidal studies, Journal of Colloid and Interface Science 179(1) (1996) 298–310.

[47]. Bansil R, Hardcastle J, Constantino M, Microrheology of mucin: tracking particles and helicobacter pylori bacteria, Epitoanyag - JSBCM 67(4) (2015) 150–154.

[48]. Olmsted SS, Padgett JL, Yudin AI, Whaley KJ, Moench TR, Cone RA, Diffusion of macromolecules and virus-like particles in human cervical mucus, Biophysical Journal 81(4) (2001) 1930–1937. [PubMed: 11566767]

[49]. Yildiz HM, McKelvey CA, Marsac PJ, Carrier RL, Size selectivity of intestinal mucus to diffusing particulates is dependent on surface chemistry and exposure to lipids, Journal of drug targeting 23(7–8) (2015) 768–774. [PubMed: 26453172]

[50]. Gonzales GB, Smagghe G, Mackie A, Grootaert C, Bajka B, Rigby N, Raes K, Van Camp J, Use of metabolomics and fluorescence recovery after photobleaching to study the bioavailability and intestinal mucus diffusion of polyphenols from cauliflower waste, Journal of Functional Foods 16 (2015) 403–413.

[51]. Wang Y-Y, Schroeder HA, Nunn KL, Woods K, Anderson DJ, Lai SK, Cone RA, Diffusion of Immunoglobulin G in Shed Vaginal Epithelial Cells and in Cell-Free Regions of Human Cervicovaginal Mucus.(Research Article), PLoS ONE 11(6) (2016) e0158338. [PubMed: 27362256]

[52]. Murgia X, Pawelzyk P, Schaefer UF, Wagner C, Willenbacher N, Lehr C-M, Size-limited penetration of nanoparticles into porcine respiratory mucus after aerosol deposition, Biomacromolecules 17(4) (2016) 1536–1542. [PubMed: 26957140]

[53]. Cu Y, Saltzman W, Controlled surface modification with poly(ethylene)glycol enhances diffusion of PLGA nanoparticles in human cervical mucus, Molecular Pharmaceutics 6(1) (2009) 173–181. [PubMed: 19053536]

[54]. Groo A-C, Saulnier P, Gimel J-C, Gravier J, Ailhas C, Benoit J-P, Lagarce F, Fate of paclitaxel lipid nanocapsules in intestinal mucus in view of their oral delivery, International Journal of Nanomedicine 8 (2013) 4291–4302. [PubMed: 24235827]

[55]. Mackie AR, Macierzanka A, Aarak K, Rigby NM, Parker R, Channell GA, Harding SE, Bajka BH, Sodium alginate decreases the permeability of intestinal mucus, Food Hydrocolloids 52 (2016) 749–755. [PubMed: 26726279]

[56]. Popov A, Enlow E, Bourassa J, Chen H, Mucus-penetrating nanoparticles made with mucoadhesive poly(vinyl alcohol), Nanomedicine: Nanotechnology, Biology, and Medicine 12(7) (2016) 1863–1871.

[57]. Mason T, Ganesan K, Vanzanten J, Wirtz D, Kuo SC, Particle tracking microrheology of complex fluids, Physical Review Letters 79(17) (1997) 3282–3285.

[58]. Crocker JC, Valentine MT, Weeks ER, Gisler T, Kaplan PD, Yodh AG, Weitz DA, Two-point microrheology of inhomogeneous soft materials, Physical Review Letters 85(4) (2000) 888–891. [PubMed: 10991424]

[59]. Yildiz H, Speciner L, Ozdemir C, Cohen D, Carrier R, Food-associated stimuli enhance barrier properties of gastrointestinal mucus, Biomaterials 54 (2015) 1–8. [PubMed: 25907034]

[60]. Macierzanka A, Mackie AR, Bajka BH, Rigby NM, Nau F, Dupont D, Transport of particles in intestinal mucus under simulated infant and adult physiological conditions: impact of mucus structure and extracellular DNA., PLOS ONE 9(4) (2014) e95274. [PubMed: 24755941]

[61]. Matthews L, Spector S, Lemm J, Potter J, The over-all chemical composition of pulmonary secretions from patients with cystic fibrosis, bronchiectasis, and laryngectomy, American Review of Respiratory Disease 88(2) (1963) 199–204. [PubMed: 14045224]

[62]. Suk JS, Lai SK, Boylan NJ, Dawson MR, Boyle MP, Hanes J, Rapid transport of muco-inert nanoparticles in cystic fibrosis sputum treated with N-acetyl cysteine., Nanomedicine 6(2) (2011) 365–375. [PubMed: 21385138]

[63]. Yildiz HM, Carlson TL, Goldstein AM, Carrier RL, Mucus barriers to microparticles and microbes are altered in Hirschsprung's disease, Macromolecular Bioscience 15(5) (2015) 712–718. [PubMed: 25644515]

[64]. Friedl H, Dünnhaupt S, Hintzen F, Waldner C, Parikh S, Pearson JP, Wilcox MD, Bernkop-Schnürch A, Development and evaluation of a novel mucus diffusion test system approved by self-nanoemulsifying drug delivery systems, Journal of Pharmaceutical Sciences 102(12) (2013) 4406–4413. [PubMed: 24258284]

[65]. Norris D, Sinko P, Effect of size, surface charge, and hydrophobicity on the translocation of polystyrene microspheres through gastrointestinal mucin, Journal of Applied Polymer Science 63(11) (1997) 1481–1492.

[66]. Boegh M, Baldursdóttir SG, Müllertz A, Nielsen HM, Property profiling of biosimilar mucus in a novel mucus-containing in vitro model for assessment of intestinal drug absorption, European Journal of Pharmaceutics and Biopharmaceutics 87(2) (2014) 227–235. [PubMed: 24413146]

[67]. Das Neves J, Rocha CMR, Gonçalves MP, Carrier RL, Amiji M, Bahia MF, Sarmento B, Interactions of microbicide nanoparticles with a simulated vaginal fluid, Molecular Pharmaceutics 9(11) (2012) 3347–3356. [PubMed: 23003680]

[68]. Larhed A, Artursson P, Björk E, The influence of intestinal mucus components on the diffusion of drugs, Pharmaceutical Research 15(1) (1998) 66–71. [PubMed: 9487548]

[69]. Yakubov GE, Papagiannopoulos A, Rat E, Waigh TA, Charge and interfacial behavior of short side-chain heavily glycosylated porcine stomach mucin, Biomacromolecules 8(12) (2007) 3791–3799. [PubMed: 17979238]

[70]. Kočevar-Nared J, Kristl J, Šmid-Korbar J, Comparative rheological investigation of crude gastric mucin and natural gastric mucus, Biomaterials 18(9) (1997) 677–681. [PubMed: 9151999]

[71]. Owen DH, Katz DF, A vaginal fluid simulant, Contraception 59(2) (1999) 91–95. [PubMed: 10361623]

[72]. Glenister DA, Salamon KE, Smith K, Beighton D, Keevil CW, Enhanced growth of complex communities of dental plaque bacteria in mucin-limited continuous culture, Microbial Ecology in Health and Disease 1(1) (1988) 31–38.

[73]. Georgiades P, Pudney PDA, Thornton DJ, Waigh TA, Particle tracking microrheology of purified gastrointestinal mucins, Biopolymers 101(4) (2014) 366–377. [PubMed: 23955640]

[74]. Savage AV, Donoghue CM, Arcy SM, Koeleman CAM, Eijnden DH, Structure determination of five sialylated trisaccharides with core types 1, 3 or 5 isolated from bovine submaxillary mucin, European Journal of Biochemistry 192(2) (1990) 427–432. [PubMed: 2209597]

[75]. Ezpeleta I, Arangoa MA, Irache JM, Stainmesse S, Chabenat C, Popineau Y, Orecchioni A-M, Preparation of Ulex europaeus lectin-gliadin nanoparticle conjugates and their interaction with gastrointestinal mucus, International Journal of Pharmaceutics 191(1) (1999) 25–32. [PubMed: 10556737]

[76]. Chayed S, Winnik FM, In vitro evaluation of the mucoadhesive properties of polysaccharide-based nanoparticulate oral drug delivery systems, European Journal of Pharmaceutics and Biopharmaceutics 65(3) (2007) 363–370. [PubMed: 17055713]

[77]. Wang Z, Xia N, Shi J, Li S, Zhao Y, Wang H, Liu L, Electrochemical aptasensor for determination of Mucin 1 by p-aminophenol redox cycling, Analytical Letters (2014).

[78]. Christersson CE, Lindh L, Arnebrant T, Film-forming properties and viscosities of saliva substitutes and human whole saliva, European Journal of Oral Sciences 108(5) (2000) 418. [PubMed: 11037758]

[79]. Sandberg T, Blom H, Caldwell KD, Potential use of mucins as biomaterial coatings. I. Fractionation, characterization, and model adsorption of bovine, porcine, and human mucins, Journal of Biomedical Materials Research Part A 91(3) (2009) 762–772. [PubMed: 19051309]

[80]. Cao X, Bansil R, Bhaskar KR, Turner BS, Lamont JT, Niu N, Afdhal NH, pH-dependent conformational change of gastric mucin leads to sol-gel transition, Biophysical Journal 76(3) (1999) 1250–1258. [PubMed: 10049309]

[81]. Smith BF, Lamont JT, Hydrophobic binding properties of bovine gallbladder mucin, The Journal of Biological Chemistry 259(19) (1984) 12170–12177. [PubMed: 6480603]

[82]. Lafitte G, Söderman O, Thuresson K, Davies J, PFG-NMR diffusometry: A tool for investigating the structure and dynamics of noncommercial purified pig gastric mucin in a wide range of concentrations, Biopolymers 86(2) (2007) 165–175. [PubMed: 17345632]

[83]. Lieleg O, Lieleg C, Bloom J, Buck CB, Ribbeck K, Mucin biopolymers as broad-spectrum antiviral agents, Biomacromolecules 13(6) (2012) 1724–1732. [PubMed: 22475261]

[84]. Celli JP, Turner BS, Afdhal NH, Ewoldt RH, McKinley GH, Bansil R, Erramilli S, Rheology of gastric mucin exhibits a pH-dependent sol-gel transition, Biomacromolecules 8(5) (2007) 1580–1586. [PubMed: 17402780]

[85]. Bansil R, Turner BS, Mucin structure, aggregation, physiological functions and biomedical applications, Current Opinion in Colloid and Interface Science 11(2) (2006) 164–170.

[86]. Carlstedt I, Lindgren H, Sheehan JK, Ulmsten U, Wingerup L, Isolation and characterization of human cervical-mucus glycoproteins, The Biochemical Journal 211(1) (1983) 13–22. [PubMed: 6409086]

[87]. Wolf DP, Sokoloski JE, Litt M, Composition and function of human cervical mucus, Biochimica et Biophysica Acta 630(4) (1980) 545–558. [PubMed: 7397238]

[88]. Xu Q, Ensign L, Boylan N, Schon A, Gong X, Yang J, Lamb N, Cai S, Yu T, Freire E, Hanes J, Impact of surface polyethylene glycol (PEG) density on biodegradable nanoparticle transport in mucus ex vivo and distribution in vivo, ACS Nano 9(9) (2015) 9217–9227. [PubMed: 26301576]

[89]. Griffiths PC, Cattoz B, Ibrahim MS, Anuonye JC, Probing the interaction of nanoparticles with mucin for drug delivery applications using dynamic light scattering, European Journal of Pharmaceutics and Biopharmaceutics 97 (2015) 218–222. [PubMed: 25986588]

[90]. Pontier C, Pachot J, Botham R, Lenfant B, Arnaud P, HT29-MTX and Caco-2/TC7 monolayers as predictive models for human intestinal absorption: role of the mucus layer, Journal of Pharmaceutical Sciences 90(10) (2001) 1608–1619. [PubMed: 11745719]

[91]. Westmoreland C, Walker T, Matthews J, Murdock J, Preliminary investigations into the use of a human bronchial cell line (16HBE14o-) to screen for respiratory toxins in vitro, Toxicology In Vitro 13(4) (1999) 761–764. [PubMed: 20654546]

[92]. Forbes B, Shah A, Martin GP, Lansley AB, The human bronchial epithelial cell line 16HBE14o− as a model system of the airways for studying drug transport, International Journal of Pharmaceutics 257(1) (2003) 161–167. [PubMed: 12711171]

[93]. Ehrhardt C, Kneuer C, Fiegel J, Hanes J, Schaefer U, Kim K-J, Lehr C-M, Influence of apical fluid volume on the development of functional intercellular junctions in the human epithelial cell line 16HBE14o- : implications for the use of this cell line as an in vitro model for bronchial drug absorption studies, Cell and Tissue Research 308(3) (2002) 391–400. [PubMed: 12107432]

[94]. Pezron I, Mitra R, Pal D, Mitra AK, Insulin aggregation and asymmetric transport across human bronchial epithelial cell monolayers (Calu-3), Journal of Pharmaceutical Sciences 91 (2002) 1135–1146. [PubMed: 11948552]

[95]. Mathia NR, Timoszyk J, Stetsko PI, Megill JR, Smith RL, Wall DA, Permeability characteristics of calu-3 human bronchial epithelial cells: in vitro-in vivo correlation to predict lung absorption in rats, Journal of drug targeting 10(1) (2002) 31–40. [PubMed: 11996084]

[96]. Witschi C, Mrsny R, In vitro evaluation of microparticles and polymer gels for use as nasal platforms for protein delivery, Pharmaceutical Research 16(3) (1999) 382–390. [PubMed: 10213368]

[97]. Fulcher ML, Gabriel S, Burns KA, Yankaskas JR, Randell SH, Well-differentiated human airway epithelial cell cultures, Methods in Molecular Medicine 107 (2005) 183–206. [PubMed: 15492373]

[98]. Hill DB, Vasquez PA, Mellnik J, McKinley SA, Vose A, Mu F, Henderson AG, Donaldson SH, Alexis NE, Boucher RC, Forest MG, A biophysical basis for mucus solids concentration as a candidate biomarker for airways disease, PLoS ONE 9(2) (2014) e87681. [PubMed: 24558372]

[99]. Lin H, Li H, Cho H-J, Bian S, Roh H-J, Lee M-K, Kim JS, Chung S-J, Shim C-K, Kim D-D, Air-Liquid Interface (ALI) Culture of Human Bronchial Epithelial Cell Monolayers as an in vitro Model for Airway Drug Transport Studies, Journal of Pharmaceutical Sciences 96 (2007) 341–350. [PubMed: 17080426]

[100]. Stewart CE, Torr EE, Mohd Jamili NH, Bosquillon C, Sayers I, Evaluation of differentiated human bronchial epithelial cell culture systems for asthma research, Journal of Allergy 2012 (2012).

[101]. Parry S, Hanisch FG, Leir S-H, Sutton-Smith M, Morris HR, Dell A, Harris A, NGlycosylation of the MUC1 mucin in epithelial cells and secretions, Glycobiology 16(7) (2006) 623–634. [PubMed: 16585136]

[102]. Huet G, Kim I, de Bolos C, Lo-Guidice JM, Moreau O, Hemon B, Richet C, Delannoy P, Real FX, Degand P, Characterization of mucins and proteoglycans synthesized by a mucin-secreting HT-29 cell subpopulation, Journal of Cell Science 108 (Pt 3) (1995) 1275–1285. [PubMed: 7622610]

[103]. Lesuffleur T, Porchet N, Aubert JP, Swallow D, Gum JR, Kim YS, Real FX, Zweibaum A, Differential expression of the human mucin genes MUC1 to MUC5 in relation to growth and differentiation of different mucus-secreting HT-29 cell subpopulations, Journal of Cell Science 106 (Pt 3) (1993) 771–783. [PubMed: 8308060]

[104]. Chen Y, Lin Y, Davis K, Wang Q, Rnjak-Kovacina J, Li CM, Isberg R, Kumamoto C, Mecsas J, Kaplan DL, Robust bioengineered 3D functional human intestinal epithelium, Scientific Reports 5 (2015).

[105]. Pan F, Han L, Zhang Y, Yu Y, Liu J, Optimization of Caco-2 and HT29 co-culture in vitro cell models for permeability studies, International Journal of Food Sciences And Nutrition 66(6) (2015) 680–685. [PubMed: 26299896]

[106]. Navabi N, McGuckin MA, Linden SK, Gastrointestinal cell lines form polarized epithelia with an adherent mucus layer when cultured in semi-wet interfaces with mechanical stimulation., PLOS ONE 8(7) (2013) e68761. [PubMed: 23869232]

[107]. Sheffner AL, The reduction in vitro in viscosity of mucoprotein solutions by a new mucolytic agent, N-acetyl-L-cysteine, Annals of the New York Academy of Sciences 106 (1963) 298–310. [PubMed: 13977050]

[108]. Behrens I, Pena A, Alonso M, Kissel T, Comparative uptake studies of bioadhesive and non-bioadhesive nanoparticles in human intestinal cell lines and rats: the effect of mucus on particle adsorption and transport, Pharmecutical Research 19(8) (2002) 1185–1193.

[109]. Gork AS, Usui N, Ceriati E, Drongowski RA, Epstein MD, Coran AG, Harmon CM, The effect of mucin on bacterial translocation in I-407 fetal and Caco-2 adult enterocyte cultured cell lines, Pediatric Surgery International 15(3) (1999) 155–159. [PubMed: 10370012]

[110]. Sato M, Sambito MA, Aslani A, Kalkhoran NM, Slamovich EB, Webster TJ, Increased osteoblast functions on undoped and yttrium-doped nanocrystalline hydroxyapatite coatings on titanium, Biomaterials 27(11) (2006) 2358–2369. [PubMed: 16337679]

[111]. In J, Foulke-Abel J, Zachos NC, Hansen A-M, Kaper JB, Bernstein HD, Halushka M, Blutt S, Estes MK, Donowitz M, Kovbasnjuk O, Enterohemorrhagic Escherichia coli reduces mucus and intermicrovillar bridges in human stem cell-derived colonoids, Cellular and Molecular Gastroenterology and Hepatology 2(1) (2016) 48–62. [PubMed: 26855967]

[112]. Bartfeld S, Clevers H, Organoids as model for infectious diseases: culture of human and murine stomach organoids and microinjection of helicobacter pylori, JoVE (105) (2015).

[113]. Moon C, Vandussen KL, Miyoshi H, Stappenbeck TS, Development of a primary mouse intestinal epithelial cell monolayer culture system to evaluate factors that modulate IgA transcytosis, Mucosal Immunology 7(4) (2013) 818–828. [PubMed: 24220295]

[114]. Vandussen KL, Marinshaw JM, Shaikh N, Miyoshi H, Moon C, Tarr PI, Ciorba MA, Stappenbeck TS, Development of an enhanced human gastrointestinal epithelial culture system to facilitate patient-based assays, Gut 64(6) (2015) 911–921. [PubMed: 25007816]

[115]. Tsamandouras N, Chen W, Edington C, Stokes C, Griffith L, Cirit M, Integrated gut and liver microphysiological systems for quantitative in vitro pharmacokinetic studies, An Official Journal of the American Association of Pharmaceutical Scientists 19(5) (2017) 1499–1512.

[116]. Chen WLK, Edington C, Suter E, Yu J, Velazquez J, Velazquez J, Shockley M, Large E, Venkataramanan R, Hughes D, Stokes C, Trumper D, Carrier RL, Cirit M, Griffith L, Lauffenburger D, Integrated gut/liver microphysiological systems elucidates inflammatory inter-tissue crosstalk, Biotechnology and Bioengineering (2017).

[117]. Maschmeyer I, Lorenz AK, Schimek K, Hasenberg T, Ramme AP, Hbner J, Lindner M, Drewell C, Bauer S, Thomas A, Sambo NS, Sonntag F, Lauster R, Marx U, A four-organ-chip for interconnected long-term co-culture of human intestine, liver, skin and kidney equivalents, Lab on a Chip 15(12) (2015) 2688–2699. [PubMed: 25996126]

[118]. Turner PV, Brabb T, Pekow C, Vasbinder MA, Administration of substances to laboratory animals: routes of administration and factors to consider, Journal of the American Association for Laboratory Animal Science 50(5) (2011) 600–613. [PubMed: 22330705]

[119]. Reardon PM, Gochoco CH, Audus KL, Wilson G, Smith PL, In vitro nasal transport across ovine mucosa: Effects of ammonium glycyrrhizinate on electrical properties and permeability of growth hormone releasing peptide, mannitol, and lucifer yellow, Pharmaceutical Research 10(4) (1993) 553–561. [PubMed: 8483838]

[120]. Wheatley MA, Dent J, Wheeldon EB, Smith PL, Nasal drug delivery: An in vitro characterization of transepithelial electrical properties and fluxes in the presence or absence of enhancers, Journal of Controlled Release 8(2) (1988) 167–177.

[121]. Smith PL, Welsh MJ, Stoff JS, Frizzell RA, Chloride secretion by canine tracheal epithelium: I. Role of intracellular cAMP levels, Journal of Membrane Biology 70(3) (1982) 217–226. [PubMed: 6313924]

[122]. Bajka B, Gillespie C, Steeb C, Read L, Howarth G, Applicability of the Ussing chamber technique to permeability determinations in functionally distinct regions of the gastrointestinal tract in the rat, Scandinavian Journal Gastroenterology 38(7) (2003) 732–41.

[123]. Smith PL, Chiossone DC, McCafferty GP, Characterization of LTC4 effects on rabbit Heal mucosa in vitro, Naunyn-Schmiedeberg's Archives of Pharmacology 341(1) (1990) 94–100.

[124]. Swaan PW, Marks GJ, Ryan FM, Smith PL, Determination of transport rates for arginine and acetaminophen in rabbit intestinal tissues in vitro, Pharmeutical Research 11(2) (1994) 283–287.

[125]. Smith PL, Lee CP, Pullen M, Ohlstein EH, Beck G, Eddy EP, Nambi P, Nonpeptide endothelin receptor antagonists: IV. Identification of receptors in rabbit colonic mucosa and smooth muscle and correlation with physiological effects, Journal of Pharmacology and Experimental Therapeutics 272(3) (1995) 1204–1210. [PubMed: 7891334]

[126]. Osbak PS, Bindslev N, Hansen MB, Relationships between body mass index and short-circuit current in human duodenal and colonic mucosal biopsies, Acta Physiologica 201(1) (2011) 47–53. [PubMed: 20950341]

[127]. Song Y, Namkung W, Nielson DW, Lee J-W, Finkbeiner WE, Verkman AS, Airway surface liquid depth measured in ex vivo fragments of pig and human trachea: dependence on Na(+) and Cl(−) channel function, American Journal of Physiology - Lung Cellular and Molecular Physiology 297(6) (2009) L1131–L1140. [PubMed: 19820035]

[128]. Griesenbach U, Soussi S, Larsen MB, Casamayor I, Dewar A, Regamey N, Bush A, Shah PL, Davies JC, Alton EWFW, Quantification of periciliary fluid height in human airway biopsies is feasible, but not suitable as a biomarker, American Journal of Respiratory Cell and Molecular Biology 44(3) (2011) 309–315. [PubMed: 20418361]

[129]. Harjeet D Sahni, Batra YK, Rajeev S, Anatomical dimensions of trachea, main bronchi, subcarinal and bronchial angles in fetuses measured ex vivo, Pediatric Anesthesia 18(11) (2008) 1029–1034. [PubMed: 18950324]

[130]. Borgmann-Winter K, Willard SL, Sinclair D, Mirza N, Turetsky B, Berretta S, Hahn CG, Translational potential of olfactory mucosa for the study of neuropsychiatric illness, Translational Psychiatry 5(3) (2015) e527. [PubMed: 25781226]

[131]. Sudhoff H, Klenke C, Greiner JFW, Müller J, Brotzmann V, Ebmeyer J, Kaltschmidt B, Kaltschmidt C, 1,8-Cineol reduces mucus-production in a novel human ex vivo model of late rhinosinusitis, PLOS ONE 10(7) (2015) e0133040. [PubMed: 26207629]

[132]. Ensign LM, Henning A, Schneider CS, Maisel K, Wang YY, Porosoff MD, Cone R, Hanes J, Ex vivo characterization of particle transport in mucus secretions coating freshly excised mucosal tissues, Molecular Pharmaceutics 10(6) (2013) 2176–2182. [PubMed: 23617606]

[133]. Ermund A, Meiss LN, Scholte BJ, Hansson GC, Hypertonic saline releases the attached small intestinal cystic fibrosis mucus, Clinical and Experimental Pharmacology & Physiology 42(1) (2015) 69–75. [PubMed: 25311799]

[134]. Johansson ME, Gustafsson JK, Holmen-Larsson J, Jabbar KS, Xia L, Xu H, Ghishan FK, Carvalho FA, Gewirtz AT, Sjovall H, Hansson GC, Bacteria penetrate the normally impenetrable inner colon mucus layer in both murine colitis models and patients with ulcerative colitis, Gut 63(2) (2014) 281–291. [PubMed: 23426893]

[135]. Zhu X, Wu J, Shan W, Zhou Z, Liu M, Huang Y, Sub-50 nm Nanoparticles with Biomimetic Surfaces to Sequentially Overcome the Mucosal Diffusion Barrier and the Epithelial Absorption Barrier, Advanced Functional Materials 26(16) (2016) 2728–2738.

[136]. Qin X, Caputo FJ, Xu D-Z, Deitch EA, Hydrophobicity of mucosal surface and its relationship to gut barrier function, Shock 29(3) (2008) 372–376. [PubMed: 17693944]

[137]. Qin X, Sheth SU, Sharpe SM, Dong W, Lu Q, Xu D, Deitch EA, The mucus layer is critical in protecting against ischemia/reperfusion-mediated gut injury and in the restitution of gut barrier function, Shock 35(3) (2011) 275–281. [PubMed: 20856173]

[138]. Karavasili C, Spanakis M, Papagiannopoulou D, Vizirianakis IS, Fatouros DG, Koutsopoulos S, Bioactive self-assembling lipid-like peptides as permeation enhancers for oral drug delivery, Journal of Pharmaceutical Sciences 104(7) (2015) 2304–2311. [PubMed: 25994901]

[139]. Lai SK, Wang Y-Y, Hida K, Cone R, Hanes J, Nanoparticles reveal that human cervicovaginal mucus is riddled with pores larger than viruses, Proceedings of the National Academy of Sciences of the United States of America 107(2) (2010) 598–603. [PubMed: 20018745]

[140]. Yasuda T, Takeyama Y, Ueda T, Shinzeki M, Sawa H, Nakajima T, Kuroda Y, Breakdown of intestinal mucosa via accelerated apoptosis increases intestinal permeability in experimental severe acute pancreatitis, Journal of Surgical Research 135(1) (2006) 18–26. [PubMed: 16603187]

[141]. Rozehnal V, Nakai D, Hoepner U, Fischer T, Kamiyama E, Takahashi M, Yasuda S, Mueller J, Human small intestinal and colonic tissue mounted in the Ussing chamber as a tool for characterizing the intestinal absorption of drugs, European Journal of Pharmaceutical Sciences 46(5) (2012) 367–373. [PubMed: 22418036]

[142]. Haslam IS, O'Reilly DA, Sherlock DJ, Kauser A, Womack C, Coleman T, Pancreatoduodenectomy as a source of human small intestine for Ussing chamber investigations and comparative studies with rat tissue, Biopharmaceutics & Drug Disposition 32(4) (2011) 210–221. [PubMed: 21416475]

[143]. Sjöberg Å, Lutz M, Tannergren C, Wingolf C, Borde A, Ungell A-L, Comprehensive study on regional human intestinal permeability and prediction of fraction absorbed of drugs using the Ussing chamber technique, European Journal of Pharmaceutical Sciences 48(1–2) (2013) 166–180. [PubMed: 23103351]

[144]. Menon RM, Barr WH, Comparison of ceftibuten transport across Caco-2 cells and rat jejunum mounted on modified ussing chambers, Biopharmaceutics & Drug Disposition 24(7) (2003) 299–308. [PubMed: 14520683]

[145]. Artursson P, Ungell A-L, Löfroth J-E, Selective paracellular permeability in two models of intestinal absorption: cultured monolayers of human intestinal epithelial cells and rat intestinal segments, Pharmaceutical Research 10(8) (1993) 1123–1129. [PubMed: 8415396]

[146]. Boisset M, Botham RP, Haegele KD, Lenfant B, Pachot JI, Absorption of angiotensin II antagonists in Ussing chambers, Caco-2, perfused jejunum loop and in vivo: Importance of drug ionisation in the in vitro prediction of in vivo absorption, European Journal of Pharmaceutical Sciences 10(3) (2000) 215–224. [PubMed: 10767599]

[147]. Kristin F, René H, Boontida M, Buraphacheep JV, Maximilian A, Johanna M, Peter L, Dissolution and dissolution/permeation experiments for predicting systemic exposure following oral administration of the BCS class II drug clarithromycin, European Journal of Pharmaceutical Sciences 101 (2017) 211–219. [PubMed: 28179133]

[148]. Gustafsson JK, Navabi N, Rodriguez-Piñeiro AM, Alomran AHA, Premaratne P, Fernandez HR, Banerjee D, Sjövall H, Hansson GC, Lindén SK, Dynamic changes in mucus thickness and ion secretion during citrobacter rodentium infection and clearance, PLOS ONE 8(12) (2013) e84430. [PubMed: 24386378]

[149]. Joly Condette C, Khorsi-Cauet H, Morlière P, Zabijak L, Reygner J, Bach V, Gay-Quéheillard J, Increased gut permeability and bacterial translocation after chronic chlorpyrifos exposure in rats, PLOS ONE 9(7) (2014) e102217. [PubMed: 25019507]

[150]. Tuvia S, Pelled D, Marom K, Salama P, Levin-Arama M, Karmeli I, Idelson GH, Landau I, Mamluk R, A novel suspension formulation enhances intestinal absorption of macromolecules via transient and reversible transport mechanisms, Pharmaceutical Research 31(8) (2014) 2010–2021. [PubMed: 24558008]

[151]. Xu Y, Wang Y, Li XM, Huang Q, Chen W, Liu R, Chen B, Wei P, Study on the release of fenofibrate nanosuspension in vitro and its correlation with in situ intestinal and in vivo absorption kinetics in rats, Drug Development and Industrial Pharmacy 40(7) (2014) 972–979. [PubMed: 23692349]

[152]. Yoo M-K, Kang S-K, Choi J-H, Park I-K, Na H-S, Lee H-C, Kim E-B, Lee N-K, Nah J-W, Choi Y-J, Cho C-S, Targeted delivery of chitosan nanoparticles to Peyer's patch using M cell-homing peptide selected by phage display technique, Biomaterials 31(30) (2010) 7738–7747. [PubMed: 20656343]

[153]. Patel JR, Barve KH, Intestinal permeability of lamivudine using single pass intestinal perfusion, Indian Journal of Pharmaceutical Sciences 74(5) (2012) 478–481. [PubMed: 23716881]

[154]. Yu T, Chan KWY, Anonuevo A, Song X, Schuster BS, Chattopadhyay S, Xu Q, Oskolkov N, Patel H, Ensign LM, van Zjil PCM, McMahon MT, Hanes J, Liposome-based mucus-penetrating particles (MPP) for mucosal theranostics: Demonstration of diamagnetic chemical exchange saturation transfer (diaCEST) magnetic resonance imaging (MRI), Nanomedicine: Nanotechnology, Biology, and Medicine 11(2) (2015) 401–405.

[155]. Ensign LM, Tang BC, Wang Y-Y, Tse TA, Hoen T, Cone R, Hanes J, Mucus-penetrating nanoparticles for vaginal drug delivery protect against herpes simplex virus, Science Translational Medicine 4(138) (2012) 138ra79.

[156]. Suk JS, Kim AJ, Trehan K, Schneider CS, Cebotaru L, Woodward OM, Boylan NJ, Boyle MP, Lai SK, Guggino WB, Hanes J, Lung gene therapy with highly compacted DNA nanoparticles that overcome the mucus barrier, Journal of Controlled Release 178 (2014) 8–17. [PubMed: 24440664]

[157]. Millet YA, Alvarez D, Ringgaard S, von Andrian UH, Davis BM, Waldor MK, Insights into Vibrio cholerae intestinal colonization from monitoring fluorescently labeled bacteria, PLOS Pathogens 10(10) (2014) e1004405. [PubMed: 25275396]

[158]. Geva-Zatorsky N, Alvarez D, Hudak JE, Reading NC, Erturk-Hasdemir D, Dasgupta S, von Andrian UH, Kasper DL, In vivo imaging and tracking of host-microbiota interactions via metabolic labeling of gut anaerobic bacteria, Nature Medicine 21(9) (2015) 1091–1100.

[159]. Kolesnikov M, Farache J, Shakhar G, Intravital two-photon imaging of the gastrointestinal tract, Journal of Immunological Methods 421 (2015) 73–80. [PubMed: 25801674]

[160]. Helmchen F, Denk W, Deep tissue two-photon microscopy, Nature Methods 2(12) (2005) 932–940. [PubMed: 16299478]

[161]. Chance B, Cope M, Gratton E, Ramanujam N, Tromberg B, Phase measurement of light absorption and scatter in human tissue, Review of Scientific Instruments 69(10) (1998) 3457–3481.

[162]. Hoover EE, Squier JA, Advances in multiphoton microscopy technology, Nature Photonics 7(2) (2013) 93–101. [PubMed: 24307915]

[163]. Ensign LM, Cone R, Hanes J, Oral drug delivery with polymeric nanoparticles: the gastrointestinal mucus barriers, Advanced drug delivery reviews 64(6) (2012) 557–570. [PubMed: 22212900]

[164]. Peterson J, Garges S, Giovanni M, McInnes P, Wang L, Schloss JA, Bonazzi V, McEwen JE, Wetterstrand KA, Deal C, Baker CC, Di Francesco V, Howcroft TK, Karp RW, Lunsford RD, Wellington CR, Belachew T, Wright M, Giblin C, David H, Mills M, Salomon R, Mullins C, Akolkar B, Begg L, Davis C, Grandison L, Humble M, Khalsa J, Little AR, Peavy H, Pontzer C, Portnoy M, Sayre MH, Starke-Reed P, Zakhari S, Read J, Watson B, Guyer M, The NIH Human Microbiome Project, Genome Research 19(12) (2009) 2317–2333. [PubMed: 19819907]

[165]. Cénit MC, Matzaraki V, Tigchelaar EF, Zhernakova A, Rapidly expanding knowledge on the role of the gut microbiome in health and disease, Biochimica et Biophysica Acta - Molecular Basis of Disease 1842(10) (2014) 1981–1992.

[166]. Garrett W, Cancer and the microbiota, Science (New York, N.Y.) 348 (2015) 80–86.

[167]. Wang J, Jia H, Metagenome-wide association studies: fine-mining the microbiome, Nature Reviews Microbiology 14(8) (2016) 508–522. [PubMed: 27396567]

[168]. Cho I, Blaser M, The human microbiome: at the interface of health and disease, Nature Reviews Genetics 13(4) (2012) 260–270.

[169]. Consortium THMP, Structure, function and diversity of the healthy human microbiome, Nature 486(7402) (2012) 207–214. [PubMed: 22699609]

[170]. Szentkuti L, Enss M-L, Comparative lectin-histochemistry on the pre-epithelial mucus layer in the distal colon of conventional and germ-free rats, Comparative Biochemistry and Physiology Part A: Molecular & Integrative Physiology 119(1) (1998) 379–386.

[171]. Comelli EM, Simmering R, Faure M, Donnicola D, Mansourian R, Rochat F, Corthesy-Theulaz I, Cherbut C, Multifaceted transcriptional regulation of the murine intestinal mucus layer by endogenous microbiota, Genomics 91(1) (2008) 70–77. [PubMed: 18035521]

[172]. Bergström A, Kristensen MB, Bahl MI, Metzdorff SB, Fink LN, Frøkiær H, Licht TR, Nature of bacterial colonization influences transcription of mucin genes in mice during the first week of life, BMC Research Notes 5 (2012) 402–402. [PubMed: 22857743]

[173]. Wrzosek L, Miquel S, Noordine M-L, Bouet S, Chevalier-Curt MJ, Robert V, Philippe C, Bridonneau C, Cherbuy C, Robbe-Masselot C, Langella P, Thomas M, Bacteroides thetaiotaomicron and Faecalibacterium prausnitzii influence the production of mucus glycans and the development of goblet cells in the colonic epithelium of a gnotobiotic model rodent, BMC Biology 11 (2013) 61. [PubMed: 23692866]

[174]. Hoskins LC, Zamcheck N, Bacterial degradation of gastrointestinal mucins, Gastroenterology 54(2) (1968) 210–217. [PubMed: 5711903]

[175]. Petersson J, Jädert C, Phillipson M, Borniquel S, Lundberg JO, Holm L, Physiological recycling of endogenous nitrate by oral bacteria regulates gastric mucus thickness, Free Radical Biology and Medicine 89 (2015) 241–247. [PubMed: 26163002]

[176]. Petersson J, Schreiber O, Hansson GC, Gendler SJ, Velcich A, Lundberg JO, Roos S, Holm L, Phillipson M, Importance and regulation of the colonic mucus barrier in a mouse model of colitis, American Journal of Physiology - Gastrointestinal and Liver Physiology 300(2) (2011) G327–G333. [PubMed: 21109593]

[177]. Besmer DM, Curry JM, Roy LD, Tinder TL, Sahraei M, Schettini J, Hwang S-I, Lee YY, Gendler SJ, Mukherjee P, Pancreatic Ductal Adenocarcinoma (PDA) mice lacking Mucin 1 have a profound defect in tumor growth and metastasis, Cancer Research 71(13) (2011) 4432–4442. [PubMed: 21558393]

[178]. Spicer AP, Rowse GJ, Lidner TK, Gendler SJ, Delayed mammary tumor progression in Muc-1 null mice, Journal of Biological Chemistry 270(50) (1995) 30093–30101. [PubMed: 8530414]

[179]. Wang HH, Afdhal NH, Gendler SJ, Wang DQ-H, Targeted disruption of the murine mucin gene 1 decreases susceptibility to cholesterol gallstone formation, Journal of Lipid Research 45(3) (2004) 438–447. [PubMed: 14703511]

[180]. Lindén SK, Sheng YH, Every AL, Miles KM, Skoog EC, Florin THJ, Sutton P, McGuckin MA, MUC1 limits Helicobacter pylori infection both by steric hindrance and by acting as a releasable decoy, PLOS Pathogens 5(10) (2009) e1000617. [PubMed: 19816567]

[181]. McGuckin MA, Every AL, Skene CD, Linden SK, Chionh YT, Swierczak A, McAuley J, Harbour S, Kaparakis M, Ferrero R, Sutton P, Muc1 mucin limits both helicobacter pylori colonization of the murine gastric mucosa and associated gastritis, Gastroenterology 133(4) (2007) 1210–1218. [PubMed: 17919495]

[182]. Banerjee D, Fernandez Harvey R., Patil Pradeep B., Premaratne P, Quiding-Järbrink M, Lindén Sara K., Epithelial MUC1 promotes cell migration, reduces apoptosis and affects levels of mucosal modulators during acetylsalicylic acid (aspirin)-induced gastropathy, Biochemical Journal 465(3) (2015) 423–431. [PubMed: 25387004]

[183]. Pastor-Soler NM, Sutton TA, Mang HE, Kinlough CL, Gendler SJ, Madsen CS, Bastacky SI, Ho J, Al-bataineh MM, Hallows KR, Singh S, Monga SP, Kobayashi H, Haase VH, Hughey RP, Muc1 is protective during kidney ischemia-reperfusion injury, American Journal of Physiology - Renal Physiology 308(12) (2015) F1452–F1462. [PubMed: 25925251]

[184]. Umehara T, Kato K, Park YS, Lillehoj EP, Kawauchi H, Kim KC, Prevention of lung injury by Muc1 mucin in a mouse model of repetitive Pseudomonas aeruginosa infection, Inflammation Research 61(9) (2012) 1013–1020. [PubMed: 22643830]

[185]. Sheng YH, Triyana S, Wang R, Das I, Gerloff K, Florin TH, Sutton P, McGuckin MA, MUC1 and MUC13 differentially regulate epithelial inflammation in response to inflammatory and infectious stimuli, Mucosal Immunology 6(3) (2013) 557–568. [PubMed: 23149663]

[186]. Guang W, Ding H, Czinn SJ, Kim KC, Blanchard TG, Lillehoj EP, Muc1 cell surface mucin attenuates epithelial inflammation in response to a common mucosal pathogen, Journal of Biological Chemistry 285(27) (2010) 20547–20557. [PubMed: 20430889]

[187]. Wang HH, Afdhal NH, Gendler SJ, Wang DQ-H, Lack of the intestinal Muc1 mucin impairs cholesterol uptake and absorption but not fatty acid uptake in Muc1−/− mice, American Journal of Physiology - Gastrointestinal and Liver Physiology 287(3) (2004) G547–G554. [PubMed: 15075252]

[188]. Nath S, Daneshvar K, Roy LD, Grover P, Kidiyoor A, Mosley L, Sahraei M, Mukherjee P, MUC1 induces drug resistance in pancreatic cancer cells via upregulation of multidrug resistance genes, Oncogenesis 2(6) (2013) e51. [PubMed: 23774063]

[189]. Zarepour M, Bhullar K, Montero M, Ma C, Huang T, Velcich A, Xia L, Vallance BA, The mucin Muc2 limits pathogen burdens and epithelial barrier dysfunction during salmonella enterica Serovar Typhimurium Colitis, Infection and Immunity 81(10) (2013) 3672–3683. [PubMed: 23876803]

[190]. Velcich A, Yang W, Heyer J, Fragale A, Nicholas C, Viani S, Kucherlapati R, Lipkin M, Yang K, Augenlicht L, Colorectal cancer in mice genetically deficient in the mucin Muc2, Science (New York, N.Y.) 295(5560) (2002) 1726–1729.

[191]. Van der Sluis M, De Koning BA, De Bruijn AC, Velcich A, Meijerink JP, Van Goudoever JB, Buller HA, Dekker J, Van Seuningen I, Renes IB, Einerhand AW, Muc2-deficient mice spontaneously develop colitis, indicating that MUC2 is critical for colonic protection, Gastroenterology 131(1) (2006) 117–129. [PubMed: 16831596]

[192]. Hartmann P, Seebauer CT, Mazagova M, Horvath A, Wang L, Llorente C, Varki NM, Brandl K, Ho SB, Schnabl B, Deficiency of intestinal mucin-2 protects mice from diet-induced fatty liver disease and obesity, American Journal of Physiology - Gastrointestinal and Liver Physiology 310(5) (2016) G310–G322. [PubMed: 26702135]

[193]. Hasnain SZ, Evans CM, Roy M, Gallagher AL, Kindrachuk KN, Barron L, Dickey BF, Wilson MS, Wynn TA, Grencis RK, Thornton DJ, Muc5ac: a critical component mediating the rejection of enteric nematodes, The Journal of Experimental Medicine 208(5) (2011) 893–900. [PubMed: 21502330]

[194]. Bergstrom KSB, Kissoon-Singh V, Gibson DL, Ma C, Montero M, Sham HP, Ryz N, Huang T, Velcich A, Finlay BB, Chadee K, Vallance BA, Muc2 protects against lethal infectious colitis by disassociating pathogenic and commensal bacteria from the colonic mucosa, PLOS Pathogens 6(5) (2010) e1000902. [PubMed: 20485566]

[195]. Wang IJ, Yu C-J, Hu F-R, Alteration of ocular surface mucins in MUC5AC-DTA transgenic mice, Molecular Vision 15 (2009) 108–119. [PubMed: 19158956]

[196]. Marko CK, Tisdale AS, Spurr-Michaud S, Evans C, Gipson IK, The ocular surface phenotype of Muc5ac and Muc5b null miceNo ocular surface phenotype in mice, Investigative Ophthalmology & Visual Science 55(1) (2014) 291–300. [PubMed: 24327612]

[197]. Floyd AM, Zhou X, Evans C, Rompala OJ, Zhu L, Wang M, Chen Y, Mucin Deficiency Causes Functional and Structural Changes of the Ocular Surface, PLOS ONE 7(12) (2012) e50704. [PubMed: 23272068]

[198]. Sheng YH, Lourie R, Lindén SK, Jeffery PL, Roche D, Tran TV, Png CW, Waterhouse N, Sutton P, Florin THJ, McGuckin MA, The MUC13 cell-surface mucin protects against intestinal inflammation by inhibiting epithelial cell apoptosis, Gut 60(12) (2011) 1661–1670. [PubMed: 21636645]

[199]. Cheon DJ, Wang Y, Deng JM, Lu Z, Xiao L, Chen CM, Bast RC, Behringer RR, CA125/MUC16 is dispensable for mouse development and reproduction, PLOS ONE 4(3) (2009) e4675. [PubMed: 19262696]

[200]. Muniyan S, Haridas D, Chugh S, Rachagani S, Lakshmanan I, Gupta S, Seshacharyulu P, Smith LM, Ponnusamy MP, Batra SK, MUC16 contributes to the metastasis of pancreatic ductal adenocarcinoma through focal adhesion mediated signaling mechanism, Genes & Cancer 7(3–4) (2016) 110–124. [PubMed: 27382435]

[201]. Shirai K, Okada Y, Cheon D-J, Miyajima M, Behringer RR, Yamanaka O, Saika S, Effects of the loss of conjunctival Muc16 on corneal epithelium and stroma in mice Muc16 and mouse cornea, Investigative Ophthalmology & Visual Science 55(6) (2014) 3626–3637. [PubMed: 24812549]

[202]. Chu HW, Rios C, Huang C, Wesolowska-Andersen A, Burchard EG, O'Connor BP, Fingerlin TE, Nichols D, Reynolds SD, Seibold MA, CRISPR-Cas9 mediated gene knockout in primary human airway epithelial cells reveals a pro-inflammatory role for MUC18, Gene Therapy 22(10) (2015) 822–829. [PubMed: 26043872]

[203]. Berman R, Jiang D, Wu Q, Stevenson CR, Schaefer NR, Chu HW, MUC18 regulates lung rhinovirus infection and inflammation, PLOS ONE 11(10) (2016) e0163927. [PubMed: 27701461]

[204]. Wu Q, Case SR, Minor MN, Jiang D, Martin RJ, Bowler RP, Wang J, Hartney J, Karimpour-Fard A, Chu HW, A novel function of MUC18: amplification of lung inflammation during bacterial infection, The American Journal of Pathology 182(3) (2013) 819–827. [PubMed: 23256918]

[205]. Stone EL, Ismail MN, Lee SH, Luu Y, Ramirez K, Haslam SM, Ho SB, Dell A, Fukuda M, Marth JD, Glycosyltransferase Function in Core 2- Type Protein O Glycosylation, Molecular and Cellular Biology 29(13) (2009) 3770–3782. [PubMed: 19349303]

[206]. Ismail MN, Stone EL, Panico M, Lee SH, Luu Y, Ramirez K, Ho SB, Fukuda M, Marth JD, Haslam SM, Dell A, High- sensitivity - glycomic analysis of mice deficient in core 2 β1,6--acetylglucosaminyltransferases, Glycobiology 21(1) (2011) 82–98. [PubMed: 20855471]

[207]. Farrell JJ, Taupin D, Koh TJ, Chen D, Zhao C-M, Podolsky DK, Wang TC, TFF2/SP- deficient mice show decreased gastric proliferation, increased acid secretion, and increased susceptibility to NSAID injury, The Journal of Clinical Investigation 109(2) (2002) 193–204. [PubMed: 11805131]

[208]. Cha HJ, Jung MS, Ahn DW, Choi JK, Ock MS, Kim KS, Yoon JH, Song EJ, Song KS, Silencing of MUC8 by siRNA increases $P2Y_2$-induced airway inflammation, American Journal of Physiology - Lung Cellular and Molecular Physiology 308(6) (2015) L495. [PubMed: 25575516]

[209]. Cha H-J, Jung M-S, Ahn DW, Choi J-K, Ock MS, Kim KS, Yoon J-H, Song EJ, Song KS, Silencing of MUC8 by siRNA increases induced airway inflammation, American Journal of Physiology - Lung Cellular and Molecular Physiology 308(6) (2015) L495. [PubMed: 25575516]

[210]. Mähler M, Bristol IJ, Leiter EH, Workman AE, Birkenmeier EH, Elson CO, Sundberg JP, Differential susceptibility of inbred mouse strains to dextran sulfate sodium-induced colitis, The American Journal of Physiology 274(3 Pt 1) (1998) G544. [PubMed: 9530156]

[211]. Vowinkel T, Kalogeris T, Mori M, Krieglstein C, Granger D, Impact of dextran sulfate sodium load on the severity of inflammation in experimental colitis, Digestive Diseases and Sciences 49(4) (2004) 556–564. [PubMed: 15185857]

[212]. Zielenski J, Rozmahel R, Bozon D, Kerem B-S, Grzelczak Z, Riordan JR, Rommens J, Tsui L-C, Genomic DNA sequence of the cystic fibrosis transmembrane conductance regulator (CFTR) gene, Genomics 10(1) (1991) 214–228. [PubMed: 1710598]

[213]. Rogers CS, Stoltz DA, Meyerholz DK, Ostedgaard LS, Rokhlina T, Taft PJ, Rogan MP, Pezzulo AA, Karp PH, Itani OA, Kabel AC, Wohlford-Lenane CL, Davis GJ, Hanfland RA, Smith TL, Samuel M, Wax D, Murphy CN, Rieke A, Whitworth K, Uc A, Starner TD, Brogden KA, Shilyansky J, McCray PB, Zabner J, Prather RS, Welsh MJ, Disruption of the CFTR gene produces a model of cystic fibrosis in newborn pigs, Science (New York, N.Y.) 321(5897) (2008) 1837–1841.

[214]. Snouwaert JN, Brigman KK, Latour AM, Malouf NN, Boucher RC, Smithies O, Koller BH, An animal model for cystic fibrosis made by gene targeting, Science (New York, N.Y.) 257(5073) (1992) 1083–1088.

[215]. Heeckeren A, Walenga R, Konstan MW, Bonfield T, Davis PB, Ferkol T, Excessive inflammatory response of cystic fibrosis mice to bronchopulmonary infection with Pseudomonas aeruginosa, The Journal of Clinical Investigation 100(11) (1997) 2810–2815. [PubMed: 9389746]

[216]. Walker WA, Pediatric gastrointestinal disease: pathophysiology, diagnosis, management, Saunders Company 2004.

[217]. Beck PL, Xavier R, Wong J, Ezedi I, Mashimo H, Mizoguchi A, Mizoguchi E, Bhan AK, Podolsky DK, Paradoxical roles of different nitric oxide synthase isoforms in colonic injury, American Journal of Physiology. Gastrointestinal and Liver Physiology 286(1) (2004) G137. [PubMed: 14665440]

[218]. Chassaing B, Aitken JD, Malleshappa M, Vijay-Kumar M, Dextran sulfate sodium (DSS)-induced colitis in mice, Current Protocols in Immunology 104(15.25) (2014) 1–14.

[219]. Venkatraman A, Ramakrishna BS, Pulimood AB, Patra S, Murthy S, Increased permeability in dextran sulphate colitis in rats: time course of development and effect of butyrate, Scandinavian Journal of Gastroenterology 35(10) (2000) 1053–1059. [PubMed: 11099058]

[220]. Ermund A, Gustafsson JK, Hansson GC, Keita AV, Mucus properties and goblet cell quantification in mouse, rat and human Ileal Peyer's patches, PLOS ONE 8(12) (2013) e83688. [PubMed: 24358305]

[221]. Allan-Wojtas P, F. ER. A solvent-based fixative for electron microscopy to improve retention and visualization of the intestinal mucus blanket for probiotic studies, Microscopy Research and Technique 36 (1997) 390–399. [PubMed: 9140941]

[222]. Shimizu T, Akamatsu T, Ota H, Katsuyama T, Immunohistochemical detection of Helicobacter pylori in the surface mucous gel layer and its clinicopathological significance, Helicobacter 1(4) (1996) 197–206. [PubMed: 9398870]

[223]. Kesimer M, Ehre C, Burns KA, Davis CW, Sheehan JK, Pickles RJ, Molecular organization of the mucins and glycocalyx underlying mucus transport over mucosal surfaces of the airways, Mucosal Immunology 6(2) (2013) 379–392. [PubMed: 22929560]

[224]. Cohen M, Varki NM, Jankowski MD, Gagneux P, Using unfixed, frozen tissues to study natural mucin distribution, JoVE (67) (2012) 3928. [PubMed: 23023050]

[225]. Ziółkowska N, Lewczuk B, Petryński W, Palkowska K, Prusik M, Targońska K, Giżejewski Z, Przybylska-Gornowicz B, Light and electron microscopy of the European beaver (castor fiber) stomach reveal unique morphological features with possible general biological significance, PLOS ONE 9(4) (2014) e94590. [PubMed: 24727802]

[226]. Fahrbach KM, Malykhina O, Stieh DJ, Hope TJ, Differential Binding of IgG and IgA to Mucus of the Female Reproductive Tract, PLOS ONE 8(10) (2013) e76176. [PubMed: 24098437]

[227]. Kobayashi K, Ogata H, Morikawa M, Iijima S, Harada N, Yoshida T, Brown WR, Inoue N, Hamada Y, Ishii H, Watanabe M, Hibi T, Distribution and partial characterisation of IgG Fc binding protein in various mucin producing cells and body fluids, Gut 51(2) (2002) 169–176. [PubMed: 12117874]

[228]. Maisel K, Ensign L, Reddy M, Cone R, Hanes J, Effect of surface chemistry on nanoparticle interaction with gastrointestinal mucus and distribution in the gastrointestinal tract following oral and rectal administration in the mouse, Journal of Controlled Release (2015) 48–57.

[229]. Chang M, Alsaigh T, Kistler EB, Schmid-Schönbein GW, Breakdown of mucin as barrier to digestive enzymes in the ischemic rat small intestine, PLOS ONE 7(6) (2012) e40087. [PubMed: 22768227]

[230]. Nichols BA, Chiappino ML, Dawson CR, Demonstration of the mucous layer of the tear film by electron microscopy, Investigative Ophthalmology & Visual Science 26(4) (1985) 464–473.

[231]. Datta SS, Preska Steinberg A, Ismagilov RF, Polymers in the gut compress the colonic mucus hydrogel, Proceedings of the National Academy of Sciences of the United States of America 113(26) (2016) 7041–7046. [PubMed: 27303035]

[232]. Jongebloed Stokroos, W. Van Der, Kalicharan, Non-coating fixation techniques or redundancy of conductive coating, low kV FE-SEM operation and combined SEM/TEM of biological tissues, Journal of Microscopy 193(2) (1999) 158–170. [PubMed: 10048219]

[233]. Kirk SE, Skepper JN, Donald AM, Application of environmental scanning electron microscopy to determine biological surface structure, Journal of Microscopy 233(2) (2009) 205–224. [PubMed: 19220687]

[234]. Ermund A, Meiss LN, Gustafsson JK, Hansson GC, Hyper-osmolarity and calcium chelation: Effects on cystic fibrosis mucus, European Journal of Pharmacology 764 (2015) 109–117. [PubMed: 26134505]

[235]. Wei X, Yang Z, Rey FE, Ridaura VK, Davidson NO, Gordon JI, Semenkovich CF, Fatty acid synthase modulates intestinal barrier function through palmitoylation of mucin 2, Cell Host & Microbe 11(2) (2012) 140–152.

[236]. Pullan RD, Thomas GA, Rhodes M, Newcombe RG, Williams GT, Allen A, Rhodes J, Thickness of adherent mucus gel on colonic mucosa in humans and its relevance to colitis, Gut 35(3) (1994) 353–359. [PubMed: 8150346]

[237]. Agrawal P, Smith D, Eng W, Cummings R, Mahal L, Large Scale Glycan Array Analysis of Commercial Lectins and Antibodies: 86 lectins and 15 antibodies, Glycobiology 22(11) (2012) 1646-1646.

[238]. Engevik MA, Yacyshyn MB, Engevik KA, Wang J, Darien B, Hassett DJ, Yacyshyn BR, Worrell RT, Human Clostridium difficile infection: altered mucus production and composition, American Journal of Physiology-Gastrointestinal and Liver Physiology 308(6) (2015) G510–G524. [PubMed: 25552581]

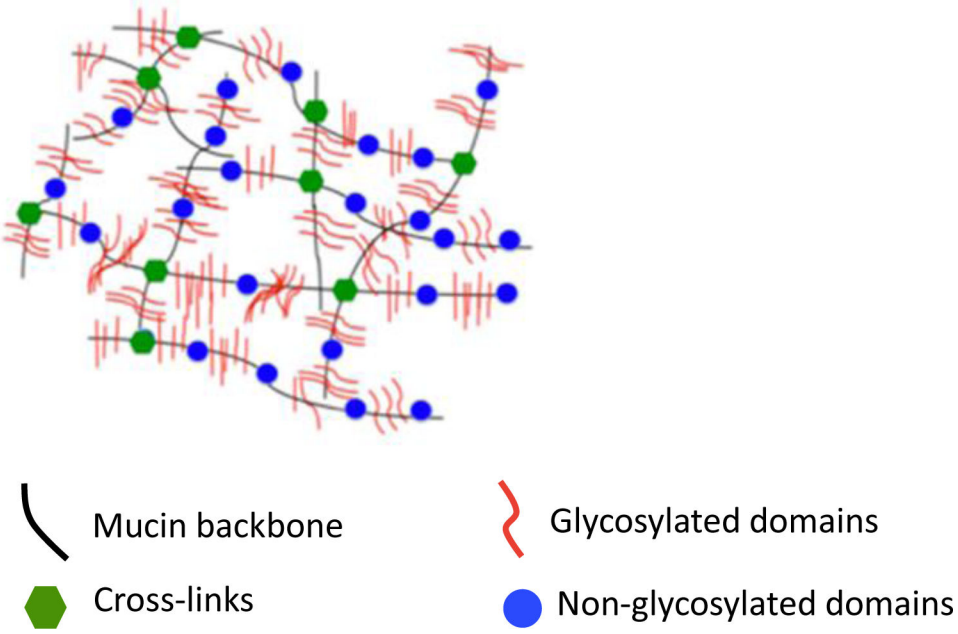

Fig. 1:

Mucin structure has both glycosylated and non-glycosylated domains along the mucin backbone. Disulfide bonds cross-link mucin monomers forming a mucin mesh-like structure[8].

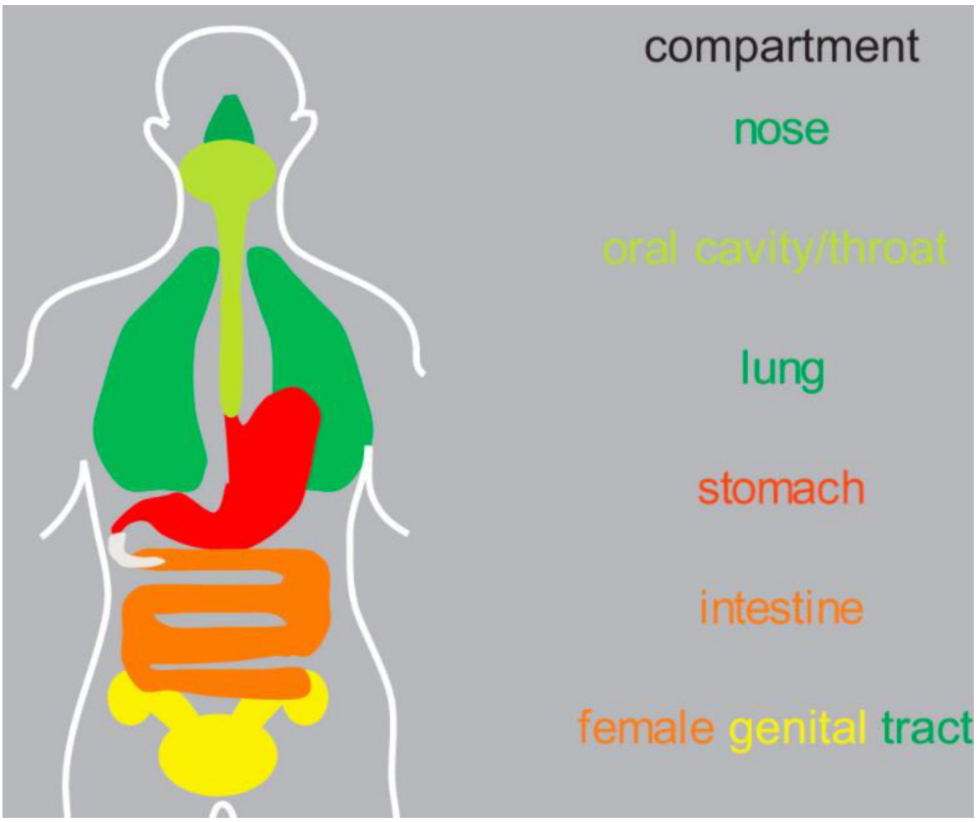

Fig. 2.
Anatomical distribution of mucus throughout the body[28].

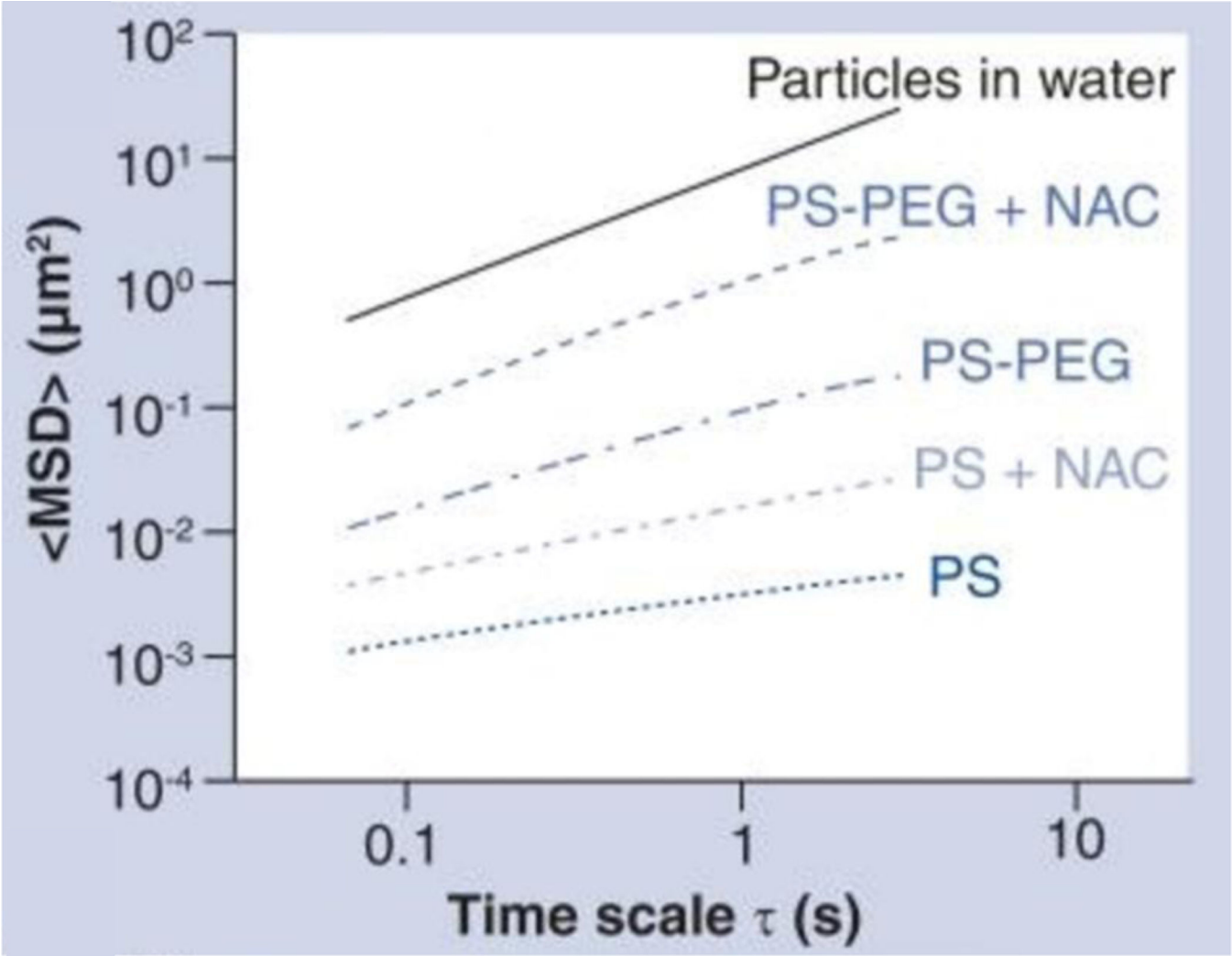

Fig. 3.

Multiple particle tracking (MPT) conducted within mucus collected from individuals with cystic fibrosis (CF) revealed that N-acetyl cysteine (NAC), a mucolytic agent, altered mucus barrier properties. MPT was used to calculate ensemble time-averaged mean squared displacement (<MSD>) vs. time scale, and demonstrated that NAC addition increased diffusion of both 200 nm carboxylate-modified (PS) and PEGylated (PS-PEG) polystyrene particles in CF mucus[62].

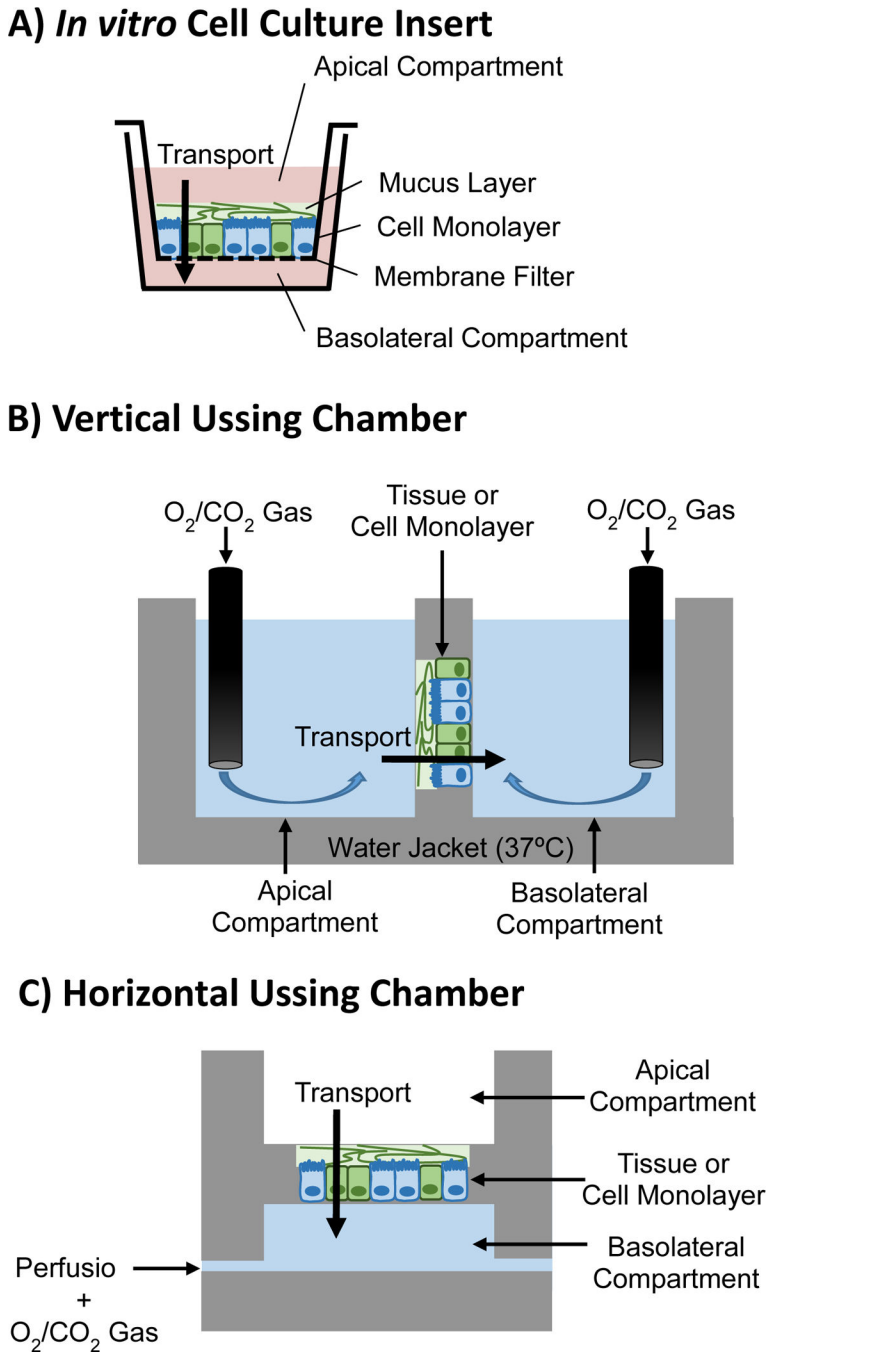

Fig. 4.

Experimental set-ups for studying drug or drug carrier transport across mucosal barriers: *in vitro* static cell culture employing a Transwell® insert (A), and tissue or cell monolayer in Ussing chamber with gas bubbling in apical and basolateral compartments in a vertical (B) configuration, or air or liquid in apical compartment and perfusion in basolateral compartment in a horizontal (C) configuration.

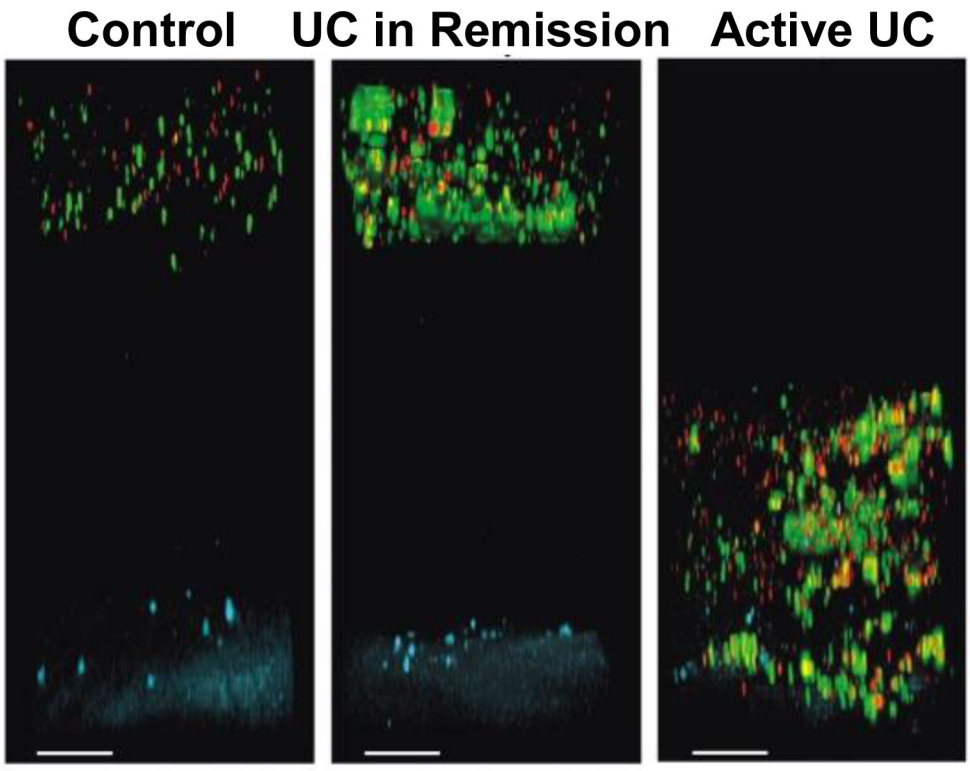

Fig. 5.

Particle penetration at the mucosal barrier of human colonic biopsy samples from controls and patients with ulcerative colitis (UC) mounted in horizontal Ussing chamber. Representative confocal Z-stack projections of 0.5 μm (red) and 2 μm (green) beads 40 minutes after addition to the colonic tissue (blue). Scale bars: 100 μm[134].

Table 1:

Different commercial sources of purified mucin.

Type	Supplier	Reported Characteristics	Literature References
Porcine stomach mucin	MyBioSource	• Partially purified mucin • 64% mucin (dry weight) • 2% solution has viscosity of 3.6 centistoke and pH 3.0–5.0	
	Orthana Kemisk Fabrik	• None available	• Characterization of molecular structure and rheological properties [69]
	Sigma (Type II)	• Crude mixture of glycoproteins • ≤ 1.2 % bound sialic acid	• Characterization of composition[70] • Diffusion experiments [44, 68] • Used in simulated vaginal mucus [67, 71]
	Sigma (Type III)	• Partially purified mucin[72] • 0.5–1.5 % bound sialic acid	• Mucin purification and characterization of composition[73]
Bovine submaxillary gland mucin	Innovative™ Research	• MW= 40–400 kDa • Protein moiety (36.6% of the molecule) • Carbohydrate moiety (56.7% of the molecule)	
	Sigma (Type I-S)	• 9–17 % bound sialic acid	• Characterization of mucin sialylated trisaccharides[74] • Characterization of particle adhesion to mucus[75, 76]
MUC1	Sino Biological	• MW= 15.4 kDa • Expressed in HEK293 cells	• Characterization of binding interaction with aptamer[77]
Artificial saliva	Orthana Kemisk Fabrik	• Composition: 3.3–3.8 g/100 mL mucin from porcine gastric lining, 100 mg/100 mL methyl-4-hydroxybenzoate, 2 mg/100 mL benzalconium chloride, 50 mg/100 mL ethylenediaminetetraacetic acid (EDTA) disodium salt • pH 5.4–7.5	• Comparison of artificial and human saliva rheological properties[78]

Table 2:

Characteristics of different mucin KO models.

KO Model	Similarities Between Muc KO and Wild Type	Characteristics Increased in Muc KO	Characteristics Decreased in Muc KO
Muc1	• Viability and fertility[178] • Muc2 and Muc4 gene expression[178] • Gallbladder size, secretion, and emptying function[179]	• Bacterial adherence to epithelium after *Helicobacter pylori* infection[180] • Wound healing rate[182, 183] • Pro-inflammatory response[176, 184–186]	• Tumor growth rate[177, 178] • Gallstone formation[179] • Drug resistance (e.g., gemcitabine, etoposide)[188] • Absorption of cholesterol[187]
Muc2	• Weight gain[190]	• Damage in intestinal injury model (e.g., dextran sulfate sodium (DSS))[191] • Onset of colorectal cancer[190] • Susceptibility to infection[189] • Mortality rate[189] • Weight loss, mortality, and colonization after *Citrobacter rodentium* infection[194] • Mucosal thickening and superficial erosions[191] • Aberrant intestinal crypt morphology, altered cell maturation and migration[190] • Pro-inflammatory response [191, 192] • Ratio of proliferating to apoptotic cells[190, 191]	• Onset of fatty liver disease and obesity with a high fat diet[192] • Epithelial barrier integrity after *Salmonella Typhimurium* infection[189]
Muc5	• External ocular appearance[195, 196] • Muc1 and Muc4 gene expression[195, 196] • Goblet cell number[196] • Number of CD45+ immune cells[196]	• Susceptibility to *Trichuris Muris* infection[193] • Late onset respiratory problems[195] • Expression of Muc5b and Muc4[195–197] • Corneal opacification[197]	• Clearance of *Trichuris Muris*[193] • Tear quality[197] • Body weight[195] • Goblet cell number[195]
Muc13	• Viability, fertility, development[198]	• Onset of acute colitis, macrophage number, and apoptosis in intestinal injury	• IL-8 expression after *Campylobacter*

KO Model	Similarities Between Muc KO and Wild Type	Characteristics Increased in Muc KO	Characteristics Decreased in Muc KO
		models (e.g., DSS) [198] • Tumor necrosis factor (TNF-α) and Interleukin (IL)-1β expression[198]	*jejuni* infection[185]
Muc16	• Viability, fertility, and development [199]	• IL-6 expression [201] • Rate of wound healing[201] • Macrophage invasion[201]	• Tumor formation and metastasis[200] • Pancreatic ductal adenocarcinoma cell proliferation, colony formation and migration *in vitro*[200] • Mucl expression[199]
Muc18		• Pro-inflammatory cytokine (KC and TNF-α) expression after Mycoplasma pneumoniae infection[204]	• Neutrophillic inflammation and viral load after humanrhino virus 1B (HRV-1B) infection[203] • IL-8 expression[202]